Title
Underscoring the Influence of Inorganic Chemistry on Nuclear Imaging with Radiometals

Journal
Inorganic Chemistry, 53(4)

ISSN
0020-1669

Authors
Zeglis, Brian M
Houghton, Jacob L
Evans, Michael J
et al.

Publication Date
2014-02-17

DOI
10.1021/ic401607z

Peer reviewed

Published in final edited form as:
Inorg Chem. 2014 February 17; 53(4): 1880–1899. doi:10.1021/ic401607z.

Underscoring the Influence of Inorganic Chemistry on Nuclear Imaging with Radiometals

Brian M. Zeglis, **Jacob L. Houghton**, **Michael J. Evans**, **Nerissa Viola-Villegas**, and **Jason S. Lewis***
Department of Radiology and the Program in Molecular Pharmacology and Chemistry, Memorial Sloan-Kettering Cancer Center, New York, New York, United States

Abstract

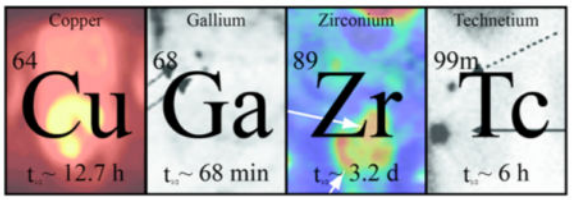

Over the past several decades, radionuclides have matured from largely esoteric and experimental technologies to indispensible components of medical diagnostics. Driving this transition, in part, have been mutually necessary advances in biomedical engineering, nuclear medicine, and cancer biology. Somewhat unsung has been the seminal role of inorganic chemistry in fostering the development of new radiotracers. In this regard, the purpose of this Forum Article is to more visibly highlight the significant contributions of inorganic chemistry to nuclear imaging by detailing the development of five metal-based imaging agents: ^{64}Cu-ATSM, ^{68}Ga-DOTATOC, ^{89}Zr-transferrin, ^{99m}Tc-sestamibi, and ^{99m}Tc-colloids. In a concluding section, several unmet needs both in and out of the laboratory will be discussed to stimulate conversation between inorganic chemists and the imaging community.

INTRODUCTION

Over the past 3 decades, nuclear imaging modalities have revolutionized clinical medicine, particularly cardiology, neurology, and oncology.[1,2] Indeed, the ability of positron emission tomography (PET) and single photon emission computed tomography (SPECT) to provide functional and biochemical information about tissues to complement the anatomical maps provided by other imaging modalities has proven vital in the diagnosis and management of disease. The advent of molecular imaging has in large part been due to remarkable advances in biomedical engineering, medical physics, halogen radiochemistry, and cancer biology. Yet the critical role of inorganic chemistry in the rise of nuclear imaging has often become

*Corresponding Author: lewisj2@mskcc.org. Phone: 1-646-888-3039. Fax: 1-646-888-3059.

Notes
The authors declare no competing financial interest.

lost in the margins. In the following pages, we will seek to remedy this oversight. We will first discuss the intersection of inorganic chemistry, radiochemistry, and nuclear imaging in general terms. Then, at greater length, we will use five particularly effective or promising metal-based imaging agents as case studies both to illustrate the fundamental role of inorganic chemistry in the development of radiopharmaceuticals and to more visibly celebrate the contributions of inorganic chemistry to nuclear imaging.

Why Use a Metallic Radioisotope?

Before we delve any deeper into our discussion, we must first answer one simple question: "Why use a metallic radioisotope?" This question becomes especially important when considering that PET imaging is largely dominated by a radiohalogen, fluorine-18 (^{18}F, $t_{1/2}$ ~ 109.8 min). The answer is straightforward: radiometals provide flexibility, modularity, and facility unmatched by other imaging isotopes.

First, the wide variety of metallic radionuclides allows for the precise tailoring of the physical half-life of the radioisotope to the biological half-life of the targeting vector (Figure 1). For example, agents with short in vivo residence times can be labeled with gallium-68 (^{68}Ga; $t_{1/2}$ ~ 68 min) or technetium-99m (^{99m}Tc; $t_{1/2}$ ~ 6 h), while vectors that require longer amounts of time to reach their target can be labeled with copper-64 (^{64}Cu; $t_{1/2}$ ~ 12.7 h), yttrium-86 (^{86}Y; $t_{1/2}$ ~ 14.7 h), indium-111 (^{111}In; $t_{1/2}$ ~ 2.8 days), or zirconium-89 (^{89}Zr; $t_{1/2}$ ~ 3.2 days) (Figure 1 and Tables 1 and 2).[3–7]

Second, the simplicity and modularity of using different bifunctional chelators and radiometals facilitate the creation of a wide variety of imaging agents. For example, with relative ease, the same antibody can be conjugated to the chelators desferrioxamine (DFO), diethylenetriaminepentaacetic acid (DTPA), and 1,4,7,10-tetraazacyclododecane-1,4,7,10-tetraacetic acid (DOTA) for labeling with ^{89}Zr for PET imaging, ^{111}In for SPECT imaging, or lutetium-177 (^{177}Lu) for radioimmunotherapy. In some cases, particularly with the versatile chelators DOTA, DTPA, and 1,4,7-triazacyclononane-1,4,7-triacetic acid (NOTA), the radiometal may be exchanged without changing the chelator at all. Either way, this modularity becomes especially clinically useful when an imaging agent labeled with one isotope can be used as a companion diagnostic tool for a therapeutic agent bearing another.[8]

Third, generally speaking, radiometalation reactions are rapid and can be achieved under mild conditions. Purification procedures are also quite simple, typically involving cation-exchange chromatography or reverse-phase C_{18} cartridges. It is in this area that radiometals likely offer the greatest advantage over radiohalogens because probes bearing the latter often require multistep syntheses, harsh reaction conditions, and complicated purifications.

Fourth, many radiometals—for example, ^{86}Y, ^{89}Zr, and ^{111}In—are known to residualize inside cells following the uptake of their vector, resulting in increased retention of the radioactivity inside the target tissue and higher tumor-to-background activity ratios than nonresidualizing radiohalogens such as ^{18}F, iodine-124 (^{124}I), and bromine-76 (^{76}Br).[9]

Finally, yet no less critically, metallic radioisotopes present a tremendous opportunity to expand the availability of imaging agents beyond hospitals with nearby cyclotron facilities

because many radiometals can be produced via portable generator systems (e.g., ^{68}Ga and ^{99m}Tc) or possess physical half-lives long enough such that they can be shipped to research laboratories and hospitals without excessive decay (e.g., ^{64}Cu, ^{111}In, and ^{89}Zr).

Production and Purification of Radiometals

The first step in the synthesis of a radiometal-based imaging agent is production of the radiometal itself. Radiometals can be produced via three distinct routes: decay of longer-lived radionuclides in a *generator*, nuclear bombardment reactions in a *cyclotron*, or nuclear bombardment reactions in a *nuclear reactor* (see Tables 1 and 2). ^{68}Ga, for example, is formed via electron capture decay of its parent radionuclide, germanium-68 (^{68}Ge), and thus can be produced using a compact, cost-effective, and convenient ^{68}Ge/^{68}Ga generator system. ^{64}Cu, in contrast, can be produced either on a nuclear reactor [via the ^{63}Cu(n,γ)^{64}Cu or ^{64}Zn(n,p)^{64}Cu reaction] or, far more commonly, by use of a biomedical cyclotron via the ^{64}Ni(p,n)^{64}Cu reaction.[10] As an aside, it is important to note that each of these isotopes emits radiation other than the positrons and photons useful for imaging. Some of these emissions, such as the variety of high-energy photons from ^{86}Y and the 909 keV photon from ^{89}Zr, require special consideration with regard to handling, shielding, and dosimetry.[11]

Yet the process does not end with the creation of the desired radiometal. The radiometal must be purified from its parent isotope and other byproducts of the nuclear reaction and isolated in a useful form prior to its incorporation into an imaging agent. Here lies the first point of intersection between inorganic chemistry and radiochemistry.

^{86}Y, for example, is most often produced via the ^{86}Sr(p,n)^{86}Y reaction by the proton bombardment of [^{86}Sr]-enriched $SrCO_3$ or SrO targets on a cyclotron. A variety of different techniques have been employed to separate the $^{86}Y^{3+}$ cation from the target and byproducts, including cation-exchange chromatography, cation-exchange chromatography followed by coprecipitation with La^{III} or Fe^{III}, and chromatography using Sr-selective resins.[12,13] Recently, a particularly effective and economical method for isolating ^{86}Y using electrolysis has been developed.[14] After irradiation of a [^{86}Sr]-enriched SrO target coated onto a platinum disk, the entire target is dissolved in nitric acid with NH_4NO_3 as an electrolyte. This solution is then placed in an electrochemical cell in which two successive rounds of electrolysis are employed to separate ^{86}Y from residual Sr via electrodeposition on a platinum-wire electrode. This ^{86}Y-coated platinum wire electrode can then be removed from the cell and washed with EtOH and HNO_3. This solution can then be evaporated and reconstituted in 0.1 M HCl to yield $^{86}Y^{3+}$ in very high specific activity and radionuclidic purity. Importantly, this method also allows for the efficient recycling of the expensive, isotopically enriched ^{86}Sr target material.

In another example, ^{89}Zr is produced via the ^{89}Y(p,n)^{89}Zr reaction by proton bombardment of a solid ^{89}Y target on a cyclotron.[15,16] In order to produce an aqueous $^{89}Zr^{4+}$ species suitable for radiolabeling reactions, the solid target is first dissolved with 6 M HCl. Yet this process produces aqueous $^{89}Zr^{4+}$ and $^{89}Y^{3+}$ species that must be separated. To this end, the HCl solution is run through a hydroxamate resin that has high affinity for $^{89}Zr^{4+}$ and very low affinity for $^{89}Y^{3+}$, thus completely sequestering the $^{89}Zr^{4+}$ cations while allowing the $^{89}Y^{3+}$ cations to pass through. Finally, $^{89}Zr^{4+}$ is removed from the hydroxamate resin

using an eluent of oxalic acid, producing a purified solution of $^{89}Zr^{4+}$ that can be employed in radiolabeling reactions.

Aqueous Coordination Chemistry of Some Common Radiometals

Prior to our discussion of metal-based imaging agents, a brief discussion of the underlying aqueous coordination chemistry of the radiometals is in order. For more detail, the reader can consult other excellent and more exhaustive reviews, chief among them a 2010 *Chemical Reviews* article from Wadas et al.[3–5,11,17–21]

To begin, four isotopes of copper have been used for PET imaging: ^{60}Cu ($t_{1/2}$ = 0.4 h; β^+ yield = 93%; $E_{\beta+}$ = 3.9 and 3.0 MeV), ^{61}Cu ($t_{1/2}$ = 3.32 h; β^+ yield = 62%; $E_{\beta+}$ = 1.2 and 1.15 MeV), ^{62}Cu ($t_{1/2}$ = 0.16 h; β^+ yield = 98%; $E_{\beta+}$ = 2.19 MeV), and, most notably, ^{64}Cu ($t_{1/2}$ = 12.7 h; β^+ yield = 19%; $E_{\beta+}$ = 0.656 MeV).[22] Of course, the chemistry of each is identical. Cu^{II} is the most biologically relevant oxidation state of the metal. Because of its electronic structure, the $3d^9$ cation typically forms square-planar four-coordinate, square-pyramidal or trigonal-bipyramidal five-coordinate, or octahedral six-coordinate complexes.[21,23] However, coordinatively saturating six-coordinate ligands have generally proven the chelators with the best in vivo performance.[3,24] Cu^{2+} is neither a particularly hard nor soft cation, so an effective chelator will almost always feature a mixture of uncharged nitrogen donors along with anionic oxygen or sulfur donors in order to neutralize the 2+ charge of the cation. While DOTA has been used as a chelator for Cu^{2+}, the Cu-DOTA complex has been shown to be unstable in vivo, often producing elevated levels of radiocopper uptake in the liver as a result of demetalation. Alternatively, other macrocyclic ligands with smaller or cross-bridged cavities, such as NOTA (N_3O_3) or 4,11-bis-(carboxymethyl)-1,4,8,11-tetrazabicyclo[6.6.2]hexadecane-4,11-di-acetic acid (CB-TE2A; N_4O_2), have been shown to be excellent chelators of the radiometal.[25–27] More recently, neutral N_6 macrocyclic chelators based on sarcophagine scaffolds have been shown to be extremely adept at chelating the cation.[28,29] The in vivo reduction of copper from Cu^{II} to Cu^{I} is possible under some circumstances. In most cases, this reduction is undesirable, and macrocyclic complexes of Cu^{II} generally have reduction potentials far below the threshold for in vivo reduction. However, in some situations, as we shall see in the Cu-ATSM case study, the reduction of Cu^{II} to Cu^{I} is a critical step in the biological mechanism of the tracer.

Moving on, the only stable oxidation state of gallium in an aqueous environment is 3+. The amphoteric nature of Ga^{3+} allows for reactions in acidic and alkaline solutions. At pH > 3, insoluble $Ga(OH)_3$ precipitates out of aqueous solutions, but this species redissolves to soluble [$Ga(OH)_4^-$] at pH > 7.4.[30] However, on the radiochemical scale, the formation of insoluble $Ga(OH)_3$ has been shown to be inconsequential if the overall radiometal concentration is kept below ~2.5×10^{-6} M.[30–32] The Ga^{3+} cation is smaller and harder than the Cu^{2+} cation and thus typically binds ligands containing multiple anionic oxygen donors.[33,34] While some tetrahedral four-coordinate and square-pyramidal five-coordinate complexes are known, octahedral six-coordinate complexes are far more common. A variety of acyclic and macrocyclic chelators have been used with Ga^{3+}, with *N*,*N*′-ethylenedi-L-cysteine (EC; $N_2S_2O_2$), *N*,*N*′-bis(2-hydroxybenzyl)ethylenediamine-*N*,*N*′-diacetic acid (HBED; N_2O_4), NOTA (N_3O_3), 1,4,7-trismercaptoethyl-1,4,7-triazacyclononane (TACN-

TM; N_3S_3), and DFO (O_6) forming particularly stable complexes.[35–38] As we will discuss later, while DOTA has been employed quite often with $^{68}Ga^{3+}$, the chelator does not form a particularly stable complex with the cation.[39] Indeed, in this regard, Ga^{3+} provides an excellent example of the importance of the cavity size of macrocyclic chelators. While NOTA binds the cation exceptionally tightly (log K = 30.1; pM = 26.4), the larger cavities of its cousins DOTA (log K = 21.3; pM = 15.2) and triethylenetetramine (TETA) (log K = 19.7; pM = 14.1) make for far less stable complexes.[40,41]

Not surprisingly, the chelation chemistry of indium is similar to that of gallium. Like its congener, indium's only stable aqueous oxidation state is 3+.[34,42] However, the In^{3+} cation is larger, has a higher pK_a, and exhibits faster water exchange rates than its Ga^{3+} counterpart.[34] As a result, In^{3+} is more tolerant of ligands bearing softer thiolate donors and can adopt higher coordination numbers than its group 13 neighbor. In part because of this flexibility, In^{3+} has been shown to form complexes with a variety of different coordination numbers and geometries. These include a five-coordinate trigonal-bipyramidal complex with tris(2-mercaptobenzyl)amine (NS_3 + an exogenous ligand), a six-coordinate distorted octahedral complex with EC ($N_2S_2O_2$), a six-coordinate distorted octahedral complex with NOTA (N_3O_3), a seven-coordinate pentagonal-bipyramidal complex with ethylenediaminetetraacetic acid (EDTA; N_2O_4 + an exogenous ligand), and an eight-coordinate square-antiprismatic complex with DTPA (N_4O_4).[36,43–48] In practice, however, the vast majority of ^{111}In-labeled bioconjugates have employed bifunctional derivatives of DTPA or DOTA.[34,42,49–52]

The biologically relevant oxidation state of yttrium is also 3+. However, the Y^{3+} cation is much larger than either Ga^{3+} or In^{3+}, allowing it to form complexes with coordination numbers up to 8 or 9. Despite its large size, the Y^{3+} cation is considered to be a hard Lewis acid, and thus ligands with multiple anionic oxygen donors are usually employed for its chelation. When a ligand offers fewer than eight donors, exogenous ligands fill the cation's coordination sphere, as in its eight-coordinate distorted dodecahedral complex with EDTA (N_2O_4 + two H_2O ligands) and nine-coordinate monocapped square-antiprismatic complex with 1,4,7-tris(carbamoylmethyl)-1,4,7-triazacyclononane (N_3O_3 + two H_2O ligands).[43,53–55] Not surprisingly, however, it has been shown that ligands capable of coordinatively saturating the metal form more stable complexes. As a result, the two chelators most often used in ^{86}Y-labeled radiopharmaceuticals both offer eight donors: DOTA forms an eight-coordinate square-antiprismatic complex with a K_d of ~22, while DTPA forms an eight-coordinate monocapped square-antiprismatic complex with a K_d of ~ 24.[49,50,52,56–60]

As a group IV metal, zirconium exists predominantly in the 4+ oxidation state in aqueous solution. The aqueous chemistry of the $Zr(H_2O)_x$ species can be quite complex, with both speciation between various mononuclear and polynuclear states and solubility highly dependent on the pH.[61–63] With regard to chelation chemistry, however, things simplify somewhat. The cation is relatively large, and its high charge makes it a very hard Lewis acid. As a result, Zr^{4+} displays a very strong preference for ligands offering anionic oxygen donors in high coordination numbers. For example, Zr^{4+} has been shown to make octadentate, dodecahedral complexes with the well-known chelators DTPA (N_3O_5), EDTA

(N_2O_4 + two H_2O ligands), and DOTA (N_4O_4).[64,65] Interestingly, however, while the thermodynamic stability constants for both Zr-EDTA (~29) and Zr-DTPA (~36) have been shown to be quite high, the poor kinetic stability of these complexes has rendered them unsuitable for use in vivo.[53,58,66] Instead, the vast majority of, if not all, published ^{89}Zr-labeled radiotracers have employed DFO as the chelator.[67–70] DFO is an acyclic siderophore-derived molecule that binds $^{89}Zr^{4+}$ using three hydroxamate groups, thus providing three neutral and three anionic oxygen ligands. To date, neither a solid state nor an NMR structure has been determined for Zr-DFO, although density functional theory (DFT) calculations suggest that a seven- or eight-coordinate complex is formed involving exogenous water molecules in addition to the ligand's six oxygen donors.[71]

Finally, the chemistry of technetium represents a fairly significant departure from the radiometals we have discussed so far. As a group VIIB metal with a neutral electronic configuration of $[Kr]4d^6 5s^1$, the coordination chemistry of ^{99m}Tc is very complex: a large number of oxidation states (1− to 7+) and a wide variety of coordination geometries (square-pyramidal, octahedral, and heptahedral) are possible.[7,18,31,72–74] This diversity is a double-edged sword: it allows for construction of a range of different ^{99m}Tc species, but it also gives rise to ample redox chemistry and chemically labile species that complicate the design of imaging agents.[75]

Upon elution from the generator as tetrahedral $^{99m}TcO_4^-$, ^{99m}Tc exists in a 7+ state that is not immediately useful for chelation or binding directly to small molecules because of its negligible chemical reactivity.[18] Indeed, there are very few examples of the incorporation of Tc^{VII} into imaging agents, with ^{99m}Tc-sulfur-colloid (Tc_2S_7) standing as the only major example.[31,76] Rather, the vast majority of ^{99m}Tc-based imaging agents are prepared using ^{99m}Tc in a lower oxidation state. As a result, a reducing agent or the direct reduction of the metal through complexation with hard ligands is necessary in the synthesis of these probes.[7,31,75]

Not surprisingly, the different oxidation states of technetium have different coordination chemistries. Tc^V is a d^2 metal center that, in aqueous environments, typically forms either five-coordinate square-pyramidal or six-coordinate octahedral complexes around a Tc^VO core or six-coordinate octahedral complexes around a Tc^VO_2 core. Ligands featuring donors ranging from neutral phosphorus and sulfur atoms to anionic oxygen atoms have been employed, although tetradentate chelators based on mercaptoacetylglycylglycylglycine, diaminedithiol, or aminoaminedithiol scaffolds have proven most common.[77,78] Complexes based on technetium(V) nitrido cores and the condensation reaction between the Tc^VO center and hydrazinonicotinamide have also been explored as alternative Tc^V coordination strategies.[79,80] Unfortunately, however, much of the work with Tc^V cores has ultimately led to complexes that are unstable or preparations that are too cumbersome for clinical translation. For example, the $^{99m}Tc^VO$ core is relatively common in radiopharmaceuticals, but these complexes are often labile at the trans position or are hydrolytically unstable when exposed to physiological environments.[31]

Low-spin Tc^{III} d^4 complexes have also been studied as alternatives to Tc^V-based constructs. The Tc^{III} center has been shown to make both six- and seven-coordinate complexes with

ligands featuring a variety of different donor types.[81,82] However, the relatively harsh reducing conditions currently employed to form Tc^{III} from pertechnetate represent a significant obstacle to its routine use.

Recently, many of the most successful developments have centered on $^{99m}Tc^{I}$, particularly complexes based on the kinetically inert, low-spin $[^{99m}Tc(CO)_3]^+$ d^6 core.[83,84] Water-soluble $[^{99m}Tc(CO)_3(H_2O)_3]^+$ can be prepared easily from ^{99m}Tc-pertechnetate under reducing conditions, and the H_2O ligands are easily exchanged with various types of ligands, including tris(pyrazoyl)methane derivatives and click-chemistry-derived scaffolds.[85–90] The lipophilicity of $[Tc(CO)_3]^+$ remains somewhat of a concern, however. Tc^{I} is a relatively soft cation, and ligands bearing softer donors tend to increase the lipophilicity of the complex further. Thus, chelation systems must be chosen carefully in order to strike a suitable balance between stability and lipophilicity.

Regardless of the identity of the metal, synthesis on the radiochemical scale has a few critical features that set it apart from the macroscale synthesis of “cold” complexes. The limited amount of time allowed for synthesis and purification is the most obvious difference, because reaction and purification conditions must often be designed with the half-life of the radionuclide in mind. A less apparent difference is the strikingly low absolute concentration of radiometals in most radiolabeling reactions. Generally, the concentration of radiometal is at least 3 (and often more) orders of magnitude lower than that of any other reactants in a radiochemical reaction. This contrasts dramatically with the excess of metal typically employed in macroscale reactions that aim to achieve the best possible chemical yield. For this reason, during radiosynthesis reactions, any potential contaminants, particularly metals that may compete with the radiometal of interest, become a major concern.

Design and Structure of Radiometal-Based Imaging Agents

From a design perspective, radiometalated imaging agents can be grouped into three classes: small metal complexes, chelator-based conjugates, and colloids. Small-metal-complex radiotracers are the most structurally straightforward class, comprised of two essential parts: a central radiometal and a set of coordinating ligands. These agents represent the purest points of intersection between inorganic chemistry and nuclear imaging, for the metal complexes themselves are solely responsible for in vivo targeting, uptake, and retention. A number of small-metal-complex PET and SPECT imaging agents have had a significant impact in the clinic, including ^{99m}Tc-bisphosphonates for bone imaging, ^{99m}Tc-sestamibi for myocardial perfusion imaging, and ^{64}Cu-PTSM for blood perfusion imaging.[6]

Chelator-based conjugates, on the other hand, have four parts: a targeting vector, a radiometal, a chelator, and a linker connecting the chelator and targeting vector.[4,5,7] The targeting vector is typically a biomolecule such as a peptide, protein, or antibody. However, synthetic vectors such as nanoparticles and liposomes have come into vogue in recent years. The selection of a radiometal is governed by both the imaging modality and the biological half-life of the targeting vector. The most popular radiometals for SPECT imaging are ^{111}In and ^{99m}Tc, and the most popular radiometals for PET imaging are ^{68}Ga, ^{64}Cu, ^{86}Y, and ^{89}Zr. However, a variety of other metallic radioisotopes including gallium-67 (^{67}Ga), copper-60 (^{60}Cu), titanium-45 (^{45}Ti), and technetium-94m (^{94m}Tc) have also been produced

and used. Once an imaging modality has been chosen, matching the radioactive half-life of the isotope to the biological half-life of the biomolecule is critical. For example, ^{68}Ga and ^{99m}Tc would not be ideal choices for labeling antibodies because the radionuclides would decay significantly before the antibody reaches its optimal concentration at the target. Conversely, neither ^{89}Zr nor ^{111}In would be the best choice for labeling a short peptide because their multiday half-lives would far exceed the residence time of the peptidic agent.

The job of the chelator—interestingly, from the Greek *χηλή* (chēlē) meaning "claw "—is simple: form a kinetically inert and thermodynamically stable complex with the radiometal in order to prevent its inadvertent release in vivo. Radiometal chelators fall into two structural classes: macrocylic and acyclic chelators. While macrocyclic chelators typically offer greater thermodynamic stability, acyclic chelators usually have faster rates of metal binding.[18] Generally, transition-metal chelators offer at least four (and usually six or more) coordinating atoms arrayed in a configuration that suits the preferred geometry of the metal in question. As we have discussed above, different metals prefer different chelators, and therefore the choice of chelator is dictated by the identity of the radiometal.

For the linkage between the chelator and targeting vector, the only requirements are that the link must be stable under physiological conditions and must not significantly compromise the binding strength or specificity of the vector. The specific chemical nature of the conjugation method is dependent on both the type of vector and the availability of bifunctional variants of the desired chelator. For vectors with free thiol groups, the reaction between a thiol and a maleimide has proven a popular route; for vectors with free amine groups, the formation of thiourea bonds using isothiocyanates or peptide bonds using activated carboxylic acids has been widely employed. It is important to remember, however, that the conjugation of a chelator to a vector may alter its ability to coordinate a given radiometal. For example, conjugating DOTA to a peptide using one of its carboxylate arms leaves only a three-armed DOTA, more properly termed DO3A, for chelation of the radiometal. In light of this, the use of bifunctional chelators with pendant conjugation handles, e.g., [*S*-2-(aminobenzyl)1,4,7-triazacyclononane-1,4,7-triacetic acid (*p*-NH_2Bn-NOTA) or *N*-(2-aminoethyl)-*trans*-1,2-diaminocyclohexane-*N*,*N*′,*N*″-pentaacetic acid (CHX-A″-DTPA), is often preferable.

The third class of radiometal-based imaging agents, colloids, is the oldest of the three, yet it boasts only one prominent example: the family of ^{99m}Tc-radiocolloids.[91–93] Nevertheless, ^{99m}Tc-radiocolloids have had a profound impact on the clinical imaging of the reticuloendothelial system (RES). Broadly speaking, colloids are particles that range in size from 1 nm to 4 μm. In the body, they are typically removed from circulation via phagocytosis, a process especially active in macrophages. Consequently, when radiolabeled, they can be used to image tissues with high concentrations of macrophages, such as the liver, spleen, bone marrow, and lymph nodes. As a result, ^{99m}Tc-radiocolloids have proven especially important in the imaging of the lymphatic system in oncology. ^{99m}Tc-colloids of a wide range of diameters have been created using a variety of materials, including denatured human albumin, sulfur, antimony, and stannous phytate. Somewhat surprisingly, the literature contains very few allusions to the use of other radiometals in colloidal imaging

agents.[94] A more detailed discussion of the synthesis and application of ^{99m}Tc-colloids can be found in the last of the five case studies.

CASE STUDIES

In the following pages, our hope is to use five metal-based radiopharmaceuticals—^{64}Cu-ATSM, ^{68}Ga-DOTATOC, ^{89}Zr-transferrin, ^{99m}Tc-sestamibi, and ^{99m}Tc-colloid—as lenses to illustrate the fundamental role of inorganic chemistry in the development of both well-established and next-generation nuclear imaging agents. Taken together, we believe that these vignettes will provide both a sound overview of the different ways inorganic chemistry influences radiopharmaceuticals and an arena for the celebration of the integral contributions of inorganic chemistry to nuclear imaging, while simultaneously pointing out areas in which inorganic chemistry could play a role moving forward.

CU-ATSM: TARGETING TUMOR PHENOTYPE WITH A SMALL METAL COMPLEX

The first PET imaging agent we will discuss is the hypoxia-targeting small-metal-complex copper(II) diacetylbis(N^4-methylthiosemicarbazone), more commonly referred to as Cu-ATSM.[95–97] Structurally, Cu-ATSM is a relatively simple metal complex: a Cu^{II} $3d^9$ metal center coordinated in a square-planar geometry by two nitrogen atoms and two sulfur atoms of a tetradentate bis(thiosemicarbazone) ligand (Figure 2A). Cu-ATSM has been radiolabeled and studied with all four positron-emitting radioisotopes of copper: ^{60}Cu, ^{61}Cu, ^{62}Cu, and ^{64}Cu. Regardless of the isotope, however, Cu-ATSM is prepared through the simple incubation of $CuCl_2$ and the free ligand H_2ATSM and purified using a reverse-phase C_{18} cartridge.

Background and In Vitro Characterization

As its name suggests, the term “hypoxia” describes the pathological condition in which a tissue is deprived of normal physiological levels of oxygen. Under normal conditions, the mean arterial partial pressure of oxygen (p_{O_2}) is 70–100 mmHg. In cancerous tissues, however, the erratic and disorganized vasculature of the growing tumor often results in dramatic reductions in p_{O_2}—in many cases to <10 mmHg and occasionally to the point of complete anoxia (0 mmHg)—with dangerous consequences for the patient.[98] Hypoxia is associated not only with significant resistance to radiation therapy but also with resistance to chemotherapies, increased tumor aggressiveness, increased metastatic potential, and higher rates of recurrence.[99,100] Given these relationships, the development of nuclear imaging tools for the noninvasive delineation of tumor hypoxia in vivo has been an incredibly important endeavor.

The selectivity of Cu-ATSM for hypoxic tissue was first discovered in 1997 using a rat model of cardiac ischemia, although it was not long until the radiotracer was applied to cancer.[101] In 1998, Dearling et al. performed a systematic study using EMT6 mouse mammary cancer cells and a series of ^{64}Cu-labeled bis(thiosemicarbazones) to determine the relationship between the ligand structure and hypoxia selectivity. In this work, the authors employed ^{64}Cu complexes of 13 different bis(thiosemicarbazone) ligands bearing structural

variations to both the diketone backbone and N-termini. From these experiments, it was concluded that Cu-ATSM displayed the greatest in vitro selectivity for hypoxic cells over their normoxic counterparts.[102] In subsequent experiments, it was discovered that ^{64}Cu-ATSM exhibited 3-fold higher retention in severely hypoxic cells compared to normal cells, a selectivity not observed with a related compound, ^{64}Cu-pyruvaldehyde-bis(*N*^{4}-methylthiosemicarbazone) (^{64}Cu-PTSM), which only differs in ligand structure by the absence of a single methyl group.[103,104]

Small-animal in vivo investigations followed soon on the heels of these in vitro studies. In one early study, using oxygen needle electrode measurements, it was found that a strong correlation exists between low p_{O_2} and high ^{64}Cu-ATSM uptake in gliosarcoma tumors in rats. Importantly, in the same study, it was shown that the chemical induction of hypoxia in a tumor could lead to a dramatic increase in ^{64}Cu-ATSM uptake.[104] In 2006, Yuan et al. used mice bearing three different types of tumors to compare the microscopic distribution of ^{64}Cu-ATSM in the tumor to that of the well-established hypoxia marker EF5.[105] The authors found that while a close correlation between the two agents could be seen in two of the tumor types, very little correlation could be seen in the third. Indeed, while a number of other investigations have illustrated strong correlations between the distribution of ^{64}Cu-ATSM uptake and that of other markers of hypoxia,[105–109] other studies illustrate instances in which little correlation can be observed.[105,106,109–112]

Mechanism

The precise mechanism responsible for Cu-ATSM's selectivity remains the subject of debate.[113] It is apparent to all, however, that the hypoxia selectivity of Cu-ATSM is predicated on two of the most fundamental tenets in inorganic chemistry: redox reactions and metal–ligand interactions. Early on, it was suggested that the difference in one-electron reduction potentials between the hypoxia-selective Cu-ATSM (−0.59 V vs Ag/AgCl) and the nonselective Cu-PTSM (−0.51 V vs Ag/AgCl) pointed to a redox-centered explanation for the phenomenon.[103] Not surprisingly, things have proven somewhat more complicated.

Given the lipophilic nature of the complex, passive diffusion is the most likely route for cell uptake. Once inside the cell, a number of different but overlapping mechanisms have been proposed to explain the selective retention of Cu-ATSM in hypoxic cells. The earliest mechanism, proposed by Fujibayashi, posited that the accumulation of Cu-ATSM in hypoxic cells is driven by the reduction of Cu^{II}-ATSM to a destabilized, d^{10} $[Cu^{I}$-ATSM$]^{-}$ complex by the hyper-reduced mitochondrial Complex 1 using NADH. This reduction is then followed by dissociation of the Cu^{+} cation from the ligand and intracellular trapping.[101] According to this scheme, hypoxia selectivity arises from the fact that in normoxic cells, Complex 1 is not in the hyper-reduced state and is thus unable to perform the reduction of Cu^{II}-ATSM, meaning the lipophilic metal complex can leave the cell unmolested. The authors argue that Cu-PTSM, on the other hand, can be reduced by Complex 1 in both normoxic *and* hypoxic cells, resulting in its failure to discriminate between hypoxic and normoxic cells.

This initial mechanistic proposal, however, was contradicted by both investigations into the uptake and washout kinetics of Cu-ATSM and the subcellular localization of the enzymes

responsible for Cu-ATSM reduction.[104,114] Therefore, a second, more sophisticated, mechanistic model was developed (Figure 2B).[102,103,115,116] This model postulates that Cu^{II}-ATSM can be reversibly reduced to $[Cu^{I}\text{-ATSM}]^{-}$ in *all* cells, likely by NADH-dependent reductases or thiol-bearing biomolecules.[113] In normoxic cells, molecular oxygen can reoxidize the complex to Cu^{II}-ATSM, restoring its planar, neutral character and allowing it to diffuse from the cell. In the low-oxygen-environment hypoxic cells, however, the reduced $[Cu^{I}\text{-ATSM}]^{-}$ complex will not be reoxidized. Instead, the complex will undergo an acid-catalyzed dissociation reaction through an intermediate such as $[Cu^{I}\text{-ATSMH}]$ or $[Cu\text{-ATSMH}_2]^{+}$, followed by the release of free H_2ATSM and the irreversible trapping of Cu^{I} in the cell, likely by thiol-bearing proteins. Thus, in this mechanism, hypoxia selectivity is related to the relative rates of oxidation, protonation, and trapping as well as the inherent stability of the reduced $[Cu^{I}\text{-ATSM}]^{-}$ complex. An abundance of experimental evidence supports this mechanism, including electrochemical, spectroscopic, crystallographic, and computational data.[102–104,113,115–120] For example, cyclic voltammetry studies clearly show that the reduction of Cu^{II}-ATSM in the acidic environment of a cancer cell would be accompanied by protonation and the generation of an unstable, diprotonated species. In addition, while the structure of a Cu^{I}-ATSM species has proven elusive, the structure of a dimeric $[Cu_2(ATSMH_2)_2]^{2+}$ has been solved, with the authors suggesting that such a species or a monomeric variant thereof could be involved in the mechanistic pathway.[121]

Significant efforts have been made to shed light on the disparity in selectivity between Cu-ATSM and Cu-PTSM. Maurer et al. suggest that the slight structural difference between the two complexes results in a shift in the relative energy levels of the metal and ligand lowest unoccupied molecular orbitals (LUMOs) of the two complexes.[116] In Cu-PTSM, the LUMO of the ligand is lower in energy than that of the metal. Therefore, the reducing electron will reside on the ligand, producing an unstable, chemically reactive triplet state, $[Cu^{II}\text{-PTSM}]^{-}$, that is prone to rapid acid-induced dissociation. In contrast, in Cu-ATSM, the LUMO of the metal is lower in energy than that of the ligand. Therefore, the reducing electron will reside on the metal and produce a singlet state, $[Cu^{I}\text{-ATSM}]^{-}$, which is both more stable and more readily reoxidized by O_2. Therefore, upon reduction, Cu-PTSM is more likely to dissociate and become trapped in the cell, whereas Cu-ATSM has a greater chance of being reoxidized and diffusing back out of the cell.

Finally, it is important to note that variations in the hypoxia selectivity of Cu-ATSM from one cell line to the next most likely stem from the network of equilibria upon which the mechanism depends. The oxidation reaction, trapping step, and any subsequent cellular transport of Cu^{I} are all subject to the proteome of the cell, and protonation of the reduced $[Cu^{I}\text{-ATSM}]$ species will depend on the intracellular pH.[109,122,123] It is well-known that both the proteome and pH of cells, particularly cancer cells, can vary significantly from cell line to cell line. It follows, then, that different cell lines could have varying capacities for the retention of Cu-ATSM. For example, the more acidic the cytoplasm of a cell, the faster the protonation of $[Cu^{I}\text{-ATSM}]$, thus increasing the amount of Cu^{I} ultimately trapped intracellularly. In the end, while it is clear that great strides have been made toward

understanding the mechanism of Cu-ATSM retention, many important questions remain, and the answers may be critical to enhancing the clinical application of the radiotracer.

Clinical Applications

Regardless of its precise mechanism, Cu-ATSM has already had a significant impact in cancer imaging. The first clinical reports of Cu-ATSM PET were published in 2000 and employed ^{62}Cu-ATSM as an imaging agent for lung cancer.[124] Since then, the majority of clinical studies have featured ^{60}Cu-ATSM, with trials focused on the potential of ^{60}Cu-ATSM as a prognostic indicator in head and neck cancer, non-small cell lung cancer, rectal carcinoma, and, most notably, cervical cancer.[125–129] One recent encouraging report detailed the slightly better target-to-muscle ratios achieved by ^{64}Cu-ATSM (7.3 ± 1.9) in comparison to ^{60}Cu-ATSM (5.9 ± 1.6) in uterocervical cancer patients (Figure 3). This result suggests that a shift toward ^{64}Cu could be beneficial and thus may significantly expand the accessibility of Cu-ATSM PET in the clinic.[98,130]

^{68}GA-DOTATOC: EVOLUTION OF CHELATOR CHOICE IN PROBE DESIGN

Our second case study, ^{68}Ga-DOTATOC, is one of the most promising metal-based tumor imaging agents currently in the clinic, and it offers a number of valuable lessons on the importance of chelators in the design of conjugate-based probes. To provide some biological context, ^{68}Ga-DOTATOC targets the somtatostatin receptor (SSTr) type 2, one of five known SSTrs. These receptors are minimally expressed in most healthy tissues, constitutively expressed at moderate levels in some organs (e.g., brain, gastrointestinal tract, pancreas, kidneys, adrenal glands, and spleen), and dramatically overexpressed in a number of malignancies, most notably neuroendocrine tumors.[131] Under normal conditions, SSTrs bind native somatostatin (SST), a multifunctional neuropeptide responsible for modulation of the secretion of hormones, including growth hormone, insulin, glucagon, and gastrin.[132] Structurally, SST is a cyclic peptide with a disulfide bridge between Cys_3 and Cys_{14} and possesses two active forms containing either 14 or 28 amino acids depending on the proteolysis of its precursor, preprosomatostatin (Figure 4A).[132] The promise of native SST for use with hormone-secreting tumors led to the development of synthetic analogues with improved in vivo stability and biological half-lives (compared to the paltry 3 min of wild-type SST).[133,134] A variant called octreotide, a cyclic octapeptide with two D-amino acid residues, was approved by the Food and Drug Administration (FDA) as a therapeutic agent for patients with hormone-secreting tumors (Figure 4B).[132,135,136] The remarkable tumor-targeting properties of this peptide spurred significant interest in using SST analogues as vehicles for the delivery of both therapeutic and diagnostic radionuclides. In response, an ^{111}In-labeled variant of octreotide—^{111}In-DTPA-octreotide (Figure 4C)—was developed and ultimately became the clinical standard radiotracer for SPECT imaging of SSTr-positive malignancies.[52,137,138]

From ^{111}In-Octreoscan to ^{68}Ga-DOTATOC

Over time, optimization of SST constructs to improve in vivo stability resulted in a shift in the chelators from DTPA to what was at the time a novel macrocyclic chelator: DOTA.[139] Indeed, ^{111}In-labeled conjugates employing DOTA displayed diminished renal toxicity and

increased tumor accumulation compared to ^{111}In-DTPA-octreotide while retaining similar overall pharmacokinetic properties.[51,139] Another trait of DOTA viewed as advantageous was its versatility with other radiometals, particularly positron-emitting ^{68}Ga. At the time, interest in using PET to image SSTr-positive malignances was on the rise, and the short half-life of ^{68}Ga (67.7 min; β^+ = 89%) makes it a nearly ideal match for peptides with rapid pharmacokinetic profiles like octreotide ($t_{1/2}$ ~100 min).[140–142]

Solid-state structures demonstrate that Ga^{3+} forms a fairly typical octahedral six-coordinate complex with DOTA, with the metal bound to the four nitrogen atoms from the macrocyclic cage and two oxygen atoms from the pendant carboxylate arms of DOTA.[143] The Ga-DOTA complex exhibits relatively modest thermodynamic stability constants (log K_{ML} ~ 21.33) and p*M* values (15.2). However, over the years, it has exhibited somewhat surprising in vivo stability in many applications.[41,46,144] Despite these limitations—indeed, almost by default—DOTA became the chelator of choice for ^{68}Ga in SSTr imaging. It has proven a successful, although slightly flawed, marriage.

Production of $^{68}Ga^{3+}$ and Synthesis of ^{68}Ga-DOTATOC

^{68}Ga is produced via electron capture decay (EC) of its parent radionuclide ^{68}Ge ($t_{1/2}$ = 270.95 days) and can thus be produced using a compact, cost-effective, and convenient generator system.[145–147] In a ^{68}Ge/^{68}Ga generator, ^{68}Ge is immobilized in a matrix of alumina, TiO_2, or SnO_2, and upon decay, $^{68}Ga^{3+}$ is formed, which has a lower affinity for the solid support than its parent and thus can be eluted in dilute acid.[145,148]

The 68-min half-life of ^{68}Ga makes radiosyntheses challenging. Most radiolabeling reactions for DOTATOC employ conditions involving heating to 90–100 °C for 5–15 min in acetate buffers or HEPES (0.1–0.5 M) with pH ranges of ~3.0–5.5 to drive the complexation reaction.[147,149–152] However, these conditions have required further optimization because of the rapid decay of the radioisotope.[131,149,150,152] Ignoring the time required for purification, a simple 15-min incubation will result in the decay of 14% of the initial radioactivity.[131,152] To circumvent this problem, Velikyan et al. explored different reaction conditions and observed that, in a microwave-assisted reaction, ^{68}Ga-DOTATOC can be synthesized in extremely high yields exceptionally rapidly: a 1-min incubation at 90 °C.[150]

As a result of ^{68}Ga's simple production, advantageous half-life, and generally favorable coordination chemistry with DOTA, ^{68}Ga-DOTA-conjugated peptides have been one of the most common classes of imaging agents reported recently. ^{68}Ga-DOTATOC, in particular, has stood as the preeminent peptide-based, receptor-targeted PET imaging probe.[153] In fact, compared to ^{111}In-DTPA-octreotide, ^{68}Ga-DOTATOC has demonstrated superior resolution as well as a greater ability to precisely measure the tumor receptor density in a number of preclinical and clinical studies (Figure 5).[149,154–156] Furthermore, ^{68}Ga-DOTATOC has proven effective for the selection of patients likely to respond to radiotherapy with ^{90}Y-DOTATOC.[157]

The Future of ^{68}Ga-Labeled Peptides: Moving Beyond "Good Enough"

A kinetically inert and thermodynamically stable radiometal–chelate complex is crucial to the success of a chelator-based radiopharmaceutical. Indeed, in vivo stability is imperative because demetalation of the radiometal can lower tumor-to-nontarget organ activity ratios, thereby decreasing contrast in imaging applications and increasing toxicity. ^{68}Ga-labeled peptides are no exception. For Ga^{3+}, trans-chelation and ligand exchange to serum apotransferrin is a particular concern because this ubiquitous protein has been shown to possess two sites with a strong affinity for Ga^{3+} (log $K_{1\text{Ga-transferrin}}$ = 20.3; log $K_{2\text{Ga-transferrin}}$ = 19.3).[30,158] Ultimately, while DOTA has been used to great effect with $^{68}Ga^{3+}$, particularly in ^{68}Ga-DOTATOC, it is not an ideal chelator for the radiometal. Simply put, DOTA is merely "good enough". The central cavity is too large to provide optimal thermodynamic stability, and its chelation kinetics are somewhat sluggish. This, in turn, requires radiolabeling reactions with either long reaction times or elevated incubation temperatures, conditions that are incompatible with both the half-life of the radionuclide and the sensitivity of some biomolecules.

In response to the limitations of DOTA, a number of novel chelators for Ga^{3+} have emerged. Likely, the best known example in the polyazamacrocycle family is NOTA (Figure 6A). NOTA is an exceptional chelator of $^{68}Ga^{3+}$.[31,159,160] The crystal structure of the Ga-NOTA complex reveals a distorted octahedral geometry with Ga^{3+} bound to the three nitrogen atoms of the ligand's annular ring and the three oxygen atoms of the pendant carboxylate arms.[159] Stability studies demonstrate that NOTA chelates Ga^{3+} with a stability constant of log K_{ML} = 30.98, almost 10 orders of magnitude higher than that of the Ga-DOTA complex.[45,161] Further, this macrocycle can be labeled with $^{68}Ga^{3+}$ at room temperature with a reaction time of ~10 min at pH 3.0–5.5, affording more mild conditions for heat-sensitive biological vectors.[147,162] The versatility of this chelator was recently illustrated using a radiolabeled octreotide conjugate. A peptide conjugated to the NOTA variant 1,4,7-triazacyclononane-1-glutaric acid-4,7-acetic acid demonstrated a high affinity for both ^{111}In and $^{68/67}$Ga, and the resulting SPECT and PET radiotracers exhibited enhanced SSTr2 targeting with improved pharmacokinetics and enhanced in vivo metabolic stability.[163]

Another macrocyclic ligand, *N*,*N*′,*N*″-triazacyclononane trisubstituted with methyl(2-carboxyethyl)phosphinic acid pendant arms (TRAP-Pr; Figure 6B), has also shown considerable promise for $^{68}Ga^{3+}$ because it can complex the cation more selectively than NOTA or DOTA.[164,165] TRAP-Pr has also been shown to bind Ga^{3+} at considerably acidic pH levels and with satisfactory kinetic inertness in a range of pH environments.[166] This trait is crucial in radiopharmaceutical kit formulations because it eliminates stabilizing ligands and cumbersome pH adjustments. Furthermore, the stability constant of TRAP-Pr with Ga^{3+} (log K_{ML} = 26.6), while lower than that of NOTA, is several orders of magnitude higher than both DOTA and apotransferrin.

A third intriguing class of Ga^{3+} chelators based on the acyclic pyridinecarboxylate-derived scaffold breaks the macrocyclic mold established by DOTA, NOTA, and TRAP. The ligand H_2dedpa (log K_{ML} = 28.11; Figure 6C), for example, achieved the highest specific activity against other chelators labeled under room temperature conditions and with no prior

purification of the ^{68}Ga eluent.[160] Further, in an apotransferrin stability challenge, ^{68}Ga-dedpa remained intact after 2 h, a result comparable to that of ^{68}Ga-NOTA. Finally, CP256 (Figure 6D) is a tris(hydroxypyridinone) ligand that rapidly (<5 min) forms a mononuclear hexadentate complex with $^{68}Ga^{3+}$ at room temperature at near physiological pH (pH ~ 6.5) with high radiochemical yields.[167]

Clearly, these alternative chelators are more suitable chelators than DOTA. It is important to remember, though, that altering a single component within a radiopharmaceutical construct is not always straightforward. Unintended consequences can arise from seemingly benign modifications. For example, the creation of a bifunctional variant of NOTA through the replacement of one of its acetate arms with a four-carbon succinic acid spacer, 1,4,7-triazacyclononane-1-succinic acid-4,7-diacetic acid (NODASA), had little effect on the stability of its complex with Ga^{3+} (log K_{ML} = 30.9).[168] Nevertheless, when this chelator was incorporated into a SSTr2-targeted agent to create ^{68}Ga-NOTATOC, decreased affinity for SSTr2 and attenuated tumor accumulation were observed compared to ^{68}Ga-DOTATOC.[169] Moreover, a seminal study by Antunes et al. illustrated that changing the metal alone even with its congeners—substituting ^{111}In for ^{68}Ga, for example—can affect the pharmacokinetics of the radiotracer for its target biomarker.[154] Thus, in the design of novel chelators for radiometals, improvements in the stability of the chelator complex must be balanced by practical considerations of the radiopharmaceutical as a whole.

^{89}ZR-TRANSFERRIN: CONTEMPORARY CHEMISTRY ENABLES NEW APPLICATIONS FOR A LONG-ESTABLISHED TUMOR-TARGETING STRATEGY

The recent development of ^{89}Zr-transferrin (^{89}Zr-Tf) stresses how a mutual appreciation of inorganic chemistry, radiochemistry, and cancer cell biology can resuscitate a venerable (but somewhat misapplied) tumor-targeting strategy. Indeed, the historically lukewarm enthusiasm for new transferrin-based radiotracers in oncology is beginning to be replaced with tentative optimism on the basis of unprecedented preclinical images with ^{89}Zr-Tf. Additionally, Tf's poor selectivity for malignant tissue (an often-cited barrier to its widespread clinical application) may now be immaterial on the basis of recent insights showing that the Tf receptor (TFRC) is regulated by at least three "druggable" oncogenes. In the following case study, both considerations will be discussed along with some concluding remarks on how to fully exploit the lessons conferred from over half a century of research on this biomolecule.

Biological Background and Previous Attempts at Nuclear Imaging with Transferrin

In order to accommodate their elevated Fe^{3+} demand, cancerous tissues generally express higher levels of TFRC than normal tissues. As a result, extensive interest has been dedicated to targeting TFRC for diagnostic and therapeutic applications.[170–172] Indeed, one of the first milestones in nuclear medicine was the discovery that $^{67}Ga^{3+}$ (a radiometal that rapidly binds Tf in serum to target TRFC) can clearly distinguish the presence or absence of lymphoma postchemotherapy where computed tomography is ambiguous.[173–176] On this

basis, several groups have attempted to modernize TFRC imaging, and Tf has been labeled with >10 different radionuclides.

Some overpowering limitations have stifled the translation of these radioconjugates for cancer imaging. Although a systematic comparison of all Tf-based radiotracers in matched tumor models is missing from the literature, an analysis of published data suggests three discouraging trends: (1) qualitative, low-resolution images representing no obvious improvement over ^{67}Ga-citrate; (2) unfavorable radiotracer catabolism in biological fluids that prevents maximal tumor contrast; (3) the use of radionuclides with half-lives not well suited to detecting TFRC expression on tumor cells.

Underscoring all of these shortcomings are the choice of radionuclide and the methodology used to attach it to Tf. An admittedly mundane example is how labeling Tf with radionuclides for SPECT (e.g., ^{99m}Tc, ^{111}In) produces images on par with ^{67}Ga-citrate and inferior to those derived from Tf adducts labeled with positron-emitting isotopes.[177–180] Less obvious are the nuances associated with how the radiolabeling strategy can impact image quality. For instance, engaging the endogenous iron binding pocket of Tf with a radiometal (e.g., $^{67/68/69}$Ga, ^{64}Cu, ^{97}Ru, ^{99m}Tc, ^{111}In, ^{113m}In) does not necessarily result in a sufficiently stable conjugate for optimal in vivo imaging of tumors.[181–191] These findings are perhaps best rationalized on the basis of Tf's avidity for Fe^{3+}: an exhaustive survey of transition metals has shown that few bind (or are predicted to bind) to Tf with the affinity of Fe^{3+}.[192,193] In this regard, cation exchange with Fe^{3+} in situ may liberate the radionuclide from Tf, resulting in rapid clearance and/or Tf-independent mechanisms of uptake in tissues. In addition, at least one Fe^{3+}-independent mechanism of Tf-radionuclide dissociation has been proposed.[194]

There are two noteworthy exceptions to this observation. Tf has been effectively coupled to iron-52 (^{52}Fe) and ^{45}Ti, two positron-emitting radionuclides with equal and higher affinity for Tf compared to Fe^{3+}, respectively.[195–199] Proof-of-concept studies in animals were also encouraging, with disease foci effectively discriminated from nearby normal tissues. Unfortunately, both radionuclides have fairly short half-lives ($t_{1/2}$ ~ 8 h for ^{52}Fe and 3 h for ^{45}Ti). In light of patient images with mAbs coupled to long-lived isotopes (e.g., ^{124}I and ^{89}Zr), the imaging community now agrees that large biomolecules (>40 kDa) are best coupled to radioisotopes with half-lives >24 h to allow image collection at later time points after injection (i.e., 3–7 days).[200–202] Consequently, what was gained in the strength of the interaction between Tf and ^{52}Fe or ^{45}Ti would likely be offset by the inability to detect the radiotracer beyond several hours after injection.

One sensible response to the aforementioned radiotracer catabolism issue is to radiolabel Tf directly via covalent modification of amino acid side chains. Two halogenated Tf adducts have been prepared by exploiting this strategy (^{18}F and ^{131}I).[203–205] As in the argument against radiolabeling Tf with ^{52}Fe and ^{45}Ti for tumor imaging, the ^{18}F-Tf adduct can be cautiously dismissed on the basis of the short half-life of ^{18}F ($t_{1/2}$ ~ 90 min). Conversely, ^{131}I has an appropriately long half-life ($t_{1/2}$ ~ 8 days), but iodination of tyrosine side chains on Tf invites the opportunity for rapid radiotracer catabolism in vivo via a different mechanism. Because Tf is internalized by a cell after binding TFRC, it is, in part,

subject to proteasomal degradation, after which free radioiodotyrosine (or free radioiodide) can be expelled. This property is not general to all radionuclides, and the community now understands that residualizing radionuclides confer better tumor contrast several days postinjection.[206] This point was shown most elegantly in a recent report comparing ^{76}Br- and ^{89}Zr-labeled METmAb (onartuzumab), an internalizing antibody to the receptor tyrosine kinase MET.[207] In this study, residualized ^{89}Zr produced more persistent images of tumors in mice compared to the nonresidualizing radioisotope bromine-76 (^{76}Br).[9]

On the basis of these observations, the case for revisiting TFRC imaging by radiolabeling Tf with ^{89}Zr became compelling for several reasons. Most importantly, the properties of ^{89}Zr are ideally suited for tumor imaging with a large biomolecule like Tf. This topic has been expertly reviewed elsewhere,[208,209] but an abridged account is that ^{89}Zr is cheaply produced from ^{89}Y (the only naturally occurring isotope of ^{89}Y), it produces positrons efficiently (23%), and, most importantly of all, its relatively long physical half-life ($t_{1/2}$ ~ 3 days) is well-suited to the biological half-life of a large biomolecule like transferrin.

^{89}Zr Chelation Chemistry: DFO and Beyond

The companion bioconjugation chemistry for ^{89}Zr is fairly robust.[11,210] As we have discussed, $^{89}Zr^{4+}$ is a highly charged, oxophilic cation that strongly prefers neutral and anionic oxygen donors to nitrogen or sulfur ligands. In recent years, the siderophore-derived chelator DFO has emerged as the primary workhorse chelator for $^{89}Zr^{4+}$. DFO is an acyclic chelator that binds $^{89}Zr^{4+}$ using three hydroxamate groups that provide three neutral and three anionic oxygen ligands, which, according to DFT calculations, are accompanied in solution by two water molecules to form an overall octadentate coordination environment (Figure 7).[71] While a variety of conjugation strategies have been reported for the attachment of DFO to biomolecules, the most common by far is the use of an isothiocyanate-modified derivative of DFO to form a thiourea linkage between the chelator and a lysine of the biomolecule in question. The subsequent radiolabeling of the DFO-modified constructs proceeds very simply and cleanly via incubation with $^{89}Zr^{4+}$ for 30–60 min at a pH of 6.5–7.5 at room temperature. Reflecting the community-wide enthusiasm for this chemistry, ~15 mAbs have been radiolabeled with ^{89}Zr-DFO and evaluated in preclinical models, with two first-in-man studies reported for ^{89}Zr-U36 and ^{89}Zr-trastuzumab.[11,210–218]

However, we would be remiss if we did not point out that DFO is not an ideal chelator for $^{89}Zr^{4+}$. Admittedly, the thermodynamic and kinetic stabilities of its complex with Zr^{4+} and its favorable radiolabeling conditions make it an extremely viable option, well beyond the “good enough” of DOTA and $^{68}Ga^{3+}$, but significant improvements can still be made. A number of preclinical in vivo studies with ^{89}Zr-DFO-labeled tracers have shown moderate levels of uptake of radioactivity (typically between 5 and 15% ID/g) in the bone, a result of the release of the osteophilic $^{89}Zr^{4+}$ cation. While similar bone uptake has not been observed in early human clinical trials of ^{89}Zr-DFO-labeled antibodies, such background uptake has the potential to be a dosimetry concern for clinicians going forward. Consequently, a number of different groups, including ours, have been working toward the development of novel, more stable chelators for ^{89}Zr. A common thread in much of this work is the creation of octodentate geometries rich in oxygen ligands, thereby reducing solvent accessibility to

the metal center and increasing stability. While no reports of new ligands have appeared in the literature as of the writing of this manuscript, we believe the next few years will witness significant strides in the development of chelators for Zr^{4+}.

Synthesis and Validation of ^{89}Zr-Tf

With these virtues in mind, our group disclosed the first synthesis and characterization of ^{89}Zr-Tf in 2012.[219] Owing to a prior report showing that Zr^{4+} does not stably bind the Fe^{3+} pockets on Tf, we chose to conjugate DFO to Tf using a bifunctional variant of DFO bearing an activated succinyl ester.[220] The synthesis of DFO-Tf was achieved in three steps following a protocol that we adapted from the literature.[70]^{89}Zr radiolabeling was consistently performed to >90% yield, and ^{89}Zr-Tf was purified using size-exclusion chromatography. As expected, ^{89}Zr-Tf was stable for >96 h in serum ex vivo and in vivo and was resistant to challenge with 10-fold excess Fe^{3+} in vitro. Its biological half-life in mice was ~118 h.

While many groups have developed Tf-based radiotracers with the intent to detect tumor tissue, we felt that recent data describing the mechanisms of TFRC regulation argued more strongly for using ^{89}Zr-Tf to monitor the treatment response to targeted therapies. Indeed, three highly visible oncogenic events regulate TFRC biology. First, TFRC is a target gene of the transcription factor MYC, an oncogenic driver of many cancers.[221–223] Second, TFRC is a target gene of the HIF1α transcription factor, which is upregulated in many tumors with PI3K pathway activation.[224–226] Finally, the kinase SRC can regulate clathrin-dependent endocytosis of the Tf-TFRC complex.[227,228] Each of these oncogenic events are immediately or distally “druggable” with targeted therapies, and given that patient response to targeted therapies is notoriously variable or short-lived, we proposed that ^{89}Zr-Tf could serve as a powerful post-therapy response indicator to quickly evaluate tumor biology.

We validated this concept by applying ^{89}Zr-Tf to MYC-driven prostate cancer models, owing to the clarity of the data linking MYC activity to TFRC expression. Remarkably, ^{89}Zr-Tf quantitatively measured treatment-induced changes in MYC (and TFRC) expression in MycCaP xenografts.[229] Moreover, ^{89}Zr-Tf detected spontaneously arising MYC-driven prostate cancer in a transgenic mouse model with prostate-specific MYC overexpression (Figure 8).[230,231] The radiotracer also detected small foci of aberrant MYC activity in mice with prostatic intraepithelial neoplasia, a clinically validated precursor to prostate cancer. On the basis of the promise of these findings, a first-in-man study for ^{89}Zr-Tf in patients with newly diagnosed prostate cancer is planned at MSKCC, and we are actively investigating the ability of ^{89}Zr-Tf to measure the pharmacological inhibition of PI3K pathway constituents and SRC in preclinical cancer models.[232,233]

Although Tf’s historical importance as a catalyst for new research in imaging is clear, that no radiotracers have achieved regulatory approval to replace ^{67}Ga-citrate for tumor targeting should provoke reflection among the chemistry and imaging communities. Because the shortcomings of experimental Tf-based radiotracers are generally related to the method of their preparation, this narrative speaks convincingly to the importance of sustained communication between inorganic chemists, radiochemists, and biologists to rationally engineer the most appropriate radiotracer for the task.

^{99M}TC-SESTAMIBI AND ^{99M}TC-COLLOIDS: USING INORGANIC CHEMISTRY TO CREATE TWO VASTLY DIFFERENT IMAGING AGENTS WITH THE SAME ISOTOPE

The final two case studies that we will discuss—^{99m}Tc-sestamibi and ^{99m}Tc-colloids—are based on the γ-emitting isotope ^{99m}Tc.[31,72,234,235] Although ^{99m}Tc was first identified in 1938, it was not until the 1960's that its potential in the development of radiopharmaceuticals was fully acknowledged and the first commercial generator technology was developed.[236,237] The production of ^{99m}Tc begins with the isolation of molybdenum-99 (^{99}Mo), which is most commonly extracted from the fission products of the neutron-irradiated uranium-235 (^{235}U) fuel from nuclear reactors. After initial processing, ^{99}Mo, in the form of molybdate (MoO_4^{2-}), is used to generate ^{99m}Tc based on theconcept of ion-exchange chromatography. $^{99}MoO_4^{2-}$ is loaded onto an acidic alumina column (Al_2O_3) that is housed inside a transportable, shielded container ("technetium cow") for distribution.[238] Upon the decay of ^{99}Mo, ^{99m}Tc-pertechnetate ($^{99m}TcO_4^{-1}$) is produced, which, because of its single charge, has a far lower affinity for alumina. Therefore, when a saline solution is flushed through the system ("milking"), $^{99m}TcO_4^-$ is eluted, while $^{99}MoO_4^{2-}$ is retained on the alumina.

^{99}Mo decays primarily through a β-decay process (~87%) that yields the metastable ^{99m}Tc, while a minor decay pathway (~13%) results in the formation of technetium-99 (^{99}Tc), a radioactive nuclide that is essentially stable ($t_{1/2}$ ~ 212000 years) and ultimately produces stable ruthenium-99 (^{99}Ru). ^{99m}Tc, in contrast, possesses a half-life of approximately 6 h and decays predominantly (>98%) via the emission of 140 keV γ-rays that are readily detected by commercially available γ-cameras for SPECT applications.[75]

^{99m}Tc-sestamibi

The most prolific radiopharmaceutical agent currently in use is ^{99m}Tc-hexakis(2-methoxy-2-methylpropyl)nitrile (^{99m}Tc-sestamibi).[239] ^{99m}Tc-sestamibi is a fairly simple metal complex composed of a coordinatively inert $^{99m}Tc^{I}$ d^6 core surrounded by an octahedral array of (2-methoxy-2-methylpropyl)nitrile ligands (Figure 9A). As a whole, ^{99m}Tc-sestamibi is lipophilic and positively charged (1+), characteristics that lead it to accumulate in the mitochondria because of its membrane permeability and the negative charge present on the inner mitochondrial matrix.[240] The contribution of the inorganic chemists who developed the series of compounds that eventually led to the discovery of ^{99m}Tc-sestamibi cannot be overstated. Many iterations of ligands were investigated, and the optimization of the physicochemical properties conferred by those ligands led to the discovery of what is currently the most commonly used imaging agent in the world today. With the radiochemistry and nuclear medicine community constantly pursuing the next great radiopharmaceutical, ^{99m}Tc-sestamibi stands as a shining example of how simple chemistry and rational design can produce an agent that can stand the test of time.

Unlike most Tc^{I} complexes that are produced via direct labeling with free ligands, ^{99m}Tc-sestamibi is produced via a ligand-exchange process using a preformed Cu^{I} complex.[75] The process begins with the reduction of pertechnetate. To this end, $^{99m}TcO_4^-$ is incubated with

a tetrakis(2-methoxyisobutylnitrile)-copper(I) tetrafluoroborate ($[Cu(MIBI)_4]^+[BF_4]^-$) complex at elevated temperature. Although the isonitriles themselves may act as reducing agents, other reducing agents are typically also added in large excess to aid in the reduction process and ensure high radiochemical yields. The reducing agent employed in commercial kits for the production of ^{99m}Tc-sestamibi is stannous chloride because it is reliable and nontoxic and the Sn^{2+} to Sn^{4+} oxidation reaction occurs with ease under the conditions for production of ^{99m}Tc-sestamibi. Additional reagents and buffers are also included in these kit formulations in order to maximize radiochemical yield.

^{99m}Tc-sestamibi has three principal applications in the clinic. The first, and most common by far, is in cardiac imaging. As a result of this mitochondrial localization, the uptake of ^{99m}Tc-sestamibi in the myocardium is directly proportional to myocardial blood flow.[241,242] Two sets of images are collected in a typical ^{99m}Tc-sestamibi cardiac SPECT procedure.[243] The first image is taken 1–1.5 h after the patient is injected with 7–10 mCi of ^{99m}Tc-sestamibi during exercise of pharmacologically induced stress. The second image is collected roughly 3 h after the first and is performed after the patient has been at rest. This two-part test allows physicians to differentiate between transient and persistent abnormalities in perfusion in the heart (Figure 9B).[244]

In addition to its widespread use as a myocardial perfusion imaging agent, ^{99m}Tc-sestamibi has also been employed in cancer imaging, most notably as a second-line diagnostic for breast cancer but also in preclinical studies of lymphoma, carcinoma, and sarcoma.[245–248] Not surprisingly, the efficacy of many chemotherapeutics is dependent upon both the amount of drug that accumulates in the tumor and the amount of time it resides there. However, the extent of accumulation and the rate of wash out are dependent on a variety of complicated factors, including blood flow, vascularization, tissue viability, and tumor metabolism. Consequently, the ability of ^{99m}Tc-sestamibi to assess perfusion has been harnessed as an indicator of the ability of a drug to reach its target. Indeed, the increased uptake and retention of ^{99m}Tc-sestamibi in tumors have in some cases been shown to be predictive of response to certain chemotherapies.[249] However, it is important to note that this story is still developing, because there are many ongoing clinical studies that aim to assess the utility of ^{99m}Tc-sestamibi as a predictive marker of treatment response.[250]

A third application of ^{99m}Tc-sestamibi is parathyroid imaging, in particular the identification and localization of adenomas in the thyroid.[251–253] Studies have shown that about 60% of hyperfunctioning parathyroids caused by the development of an adenoma will accumulate ^{99m}Tc-sestamibi more quickly than normal parathyroid glands.[251–253] For this application, SPECT images are obtained shortly after injection to identify all glands, and images are obtained again after the tracer has been allowed to wash out, allowing for identification of the abnormal glands.

In more recent years, the field of ^{99m}Tc chemistry has unquestionably witnessed a number of important advances, including developments in ^{99m}Tc-tricarbonyl chemistry (including kit-based formulations), the use of hydrazinonicatinomide for ^{99m}TcO-based labelings, and the creation of the clever “click-to-chelate” radiolabeling methodology. In this regard, the work of Alberto and Schibli in Switzerland, Blower in the U.K., and Jurisson in the U.S. has

been particularly important.[19,20,83,84,87,254–256] However, despite these successes, it is hard to avoid the impression that progress in the field as a whole seems to have slowed somewhat in recent years. The overall lack of new complexes, novel chelators, and effective and biologically stable ^{99m}Tc-based bioconjugates highlights the need for fresh ideas and new avenues of research.

^{99m}Tc-colloids

While ^{99m}Tc-sestamibi is the product of the careful manipulation of the chemical properties conferred by ligands, the chemistry of ^{99m}Tc-colloids is much less well-defined. That said, while the chemistry and biological targets of colloids are very different from other classes of radiopharmaceuticals, their impact on nuclear imaging has been significant. Indeed, in recent decades, ^{99m}Tc-colloids have undergone numerous iterative developments and have been approved for numerous applications.

Generally speaking, colloids are particles of a certain size range (1 nm to 4 μm) that mimic the types of particles found in human body fluids that are removed by macrophages via phagocytosis.[257] The majority of the macrophage population in humans is found in the RES, which is comprised of the lymph nodes, bone marrow, liver, and spleen. Sites of infection and inflammation also experience increases in macrophage populations. In addition to the particle size, a number of other features determine the biological fate of ^{99m}Tc-colloids and their potential imaging applications, including their charge and potential to interact with biological macromolecules. As a result, a wide variety of formulations have been used to create ^{99m}Tc-colloids, including ^{99m}Tc-tin-colloid (Amerscan Hepatate II), ^{99m}Tc-rhenium-sulfide-colloid (Sulfotec), and ^{99m}Tc-albumin-microcolloid (Microlite).

Relative to ^{99m}Tc-based small metal complexes and bioconjugates, the radiochemistry of ^{99m}Tc-colloids varies greatly, and the self-assembly process, while tunable, is somewhat poorly defined. For example, production of ^{99m}Tc-tin-fluoride-colloids, which have been used to label leukocytes in vitro, proceeds from small “template” particles that are formed by nucleation from a supersaturated solution of reagents, including tin(II) fluoride, sodium fluoride, ^{99m}Tc, and polaxamer 188 (a stabilizing agent).[258,259] Those template particles then grow from the remaining reactants in the solution, capturing the technetium atoms within the macromolecular complex in a self-assembly process that can be tuned by physical manipulation of the solution.[260] Factors that may influence the formation of the colloid include the pH, incubation time, length and degree of agitation, and the shear force from drawing the solution into a syringe. These factors can affect the size of the particles, which can, in turn, influence their biological activity.

In contrast, a very different type of radiochemistry is used in the production of ^{99m}Tc-albumin-nanocolloid (Microlite), which is commonly used for lymphoscintigraphy, bone marrow scintigraphy, and inflammation scintigraphy.[94] In this case, the albumin provides a “template” for the radiocolloid, which is not as sensitive to physical manipulation. As a result, ^{99m}Tc-albumin-nanocolloid can be produced in more uniform particle sizes. The synthesis of ^{99m}Tc-albumin-nanocolloid is achieved by simply reducing ^{99m}Tc-pertechnetate with $SnCl_2$ and then mixing it with a preformed human serum albumin aggregate at room temperature.

One of the primary uses of ^{99m}Tc-colloids is lymphoscintigraphy, particularly sentinel lymph node mapping (Figure 10).[261–263] Sentinel lymph nodes are the first node or group of nodes that receive drainage from a tumor and, as a result, are particularly prone to metastatic spread. When injected at the site of a tumor, ^{99m}Tc-colloids will follow the route of lymphatic drainage because they are too large to enter the bloodstream and will be consumed by resident macrophages upon reaching the sentinel lymph node. Once the process is complete, delineation of the lymph nodes via SPECT imaging is possible. How well a particular colloid localizes at a sentinel lymph node is determined by its size: particles in the 200–300 nm range typically will be retained in the first lymph node, whereas smaller particles tend to migrate farther and more rapidly through the lymphatic system, a characteristic that may be desirable depending on the procedure.[257,262] Biopsy or radio-guided resection of the sentinel lymph node is often the goal, in which case a colloid is chosen to balance the speed of migration and amount of phagocytosis.

In the end, although the chemistry of many ^{99m}Tc-colloids is not particularly well elucidated, they have become an indispensable radiopharmaceutical in the clinic. That said, the chemistry and mechanism of these probes warrant further investigation to prevent the field from falling into an ill-advised sense of "*if it ain't broke, don't fix it*". Such information should allow more precise fine-tuning of the particle size and shape, which, in turn, will allow for the ab initio development of particles that serve more precise applications in the future.

FRONTIERS FOR INORGANIC CHEMISTRY AND NUCLEAR IMAGING: THE YEARS AHEAD

Up to this point, we have sought predominantly to highlight the tremendous impact of inorganic chemistry on nuclear medicine. However, we also feel it is important to address a number of the challenges faced by the two fields in the years to come. Indeed, we believe that the relationship between inorganic chemistry and nuclear imaging has never been more important. The use of radiometals in nuclear imaging currently lies at an incredibly important juncture, with the number of radiometal-based imaging agents in clinical trials at an all-time high and ^{68}Ga-DOTATOC on the cusp of FDA approval in the United States. Expectations—and standards—have never been higher, and a concerted effort between inorganic chemists, radiochemists, and nuclear imaging scientists will be essential in order to move metal-based radiopharmaceuticals forward. These challenges can be loosely organized into two groups, lying outside and inside the laboratory.

Growth Outside the Laboratory

1. Broadening the Availability of Radiometals—The first obstacle, and one that lies more in the purview of politicians and administrators than scientists, is the lack of widespread availability of many radiometals, a problem reinforced by the worldwide shortage of ^{99m}Tc that started just a few years ago and continues today. The American Medical Isotope Production Act signed into law this past January will do much to alleviate concerns over ^{99m}Tc in the United States. However, both imaging radiometals such as ^{64}Cu, ^{89}Zr, and ^{111}In and therapeutic radiometals such as ^{177}Lu and ^{225}Ac are still only

produced in a handful of facilities worldwide, and this scarcity—both literal because of geographical logistics and practical because of high costs—hinders both the preclinical development and clinical utilization of radiometal-based imaging agents.

2. Building Bridges between Inorganic Chemistry and Nuclear Medicine— Second, it is imperative that stronger links be formed between the inorganic chemistry, radiochemistry, and nuclear imaging communities. One particularly powerful way to do this is to more fully integrate radiochemistry and nuclear imaging into the inorganic chemistry curricula of undergraduate and graduate chemistry departments. In addition, facilitating radiochemical research in university chemistry departments—rather than in medical centers, where it is now largely stationed—would ensure a generation of radiochemists and molecular imaging researchers that are well-trained in the fundamentals of inorganic chemistry. This would no doubt require investment, in terms of both facilities and personnel. However, the returns, in the form of better-trained students and productive collaborations, would almost certainly justify the outlays, particularly in light of the emphasis currently being placed on translational science by preeminent funding agencies. Finally, better incorporation of radiochemistry and nuclear imaging into chemistry conferences could facilitate the exchange of ideas. For example, while the annual meeting of the American Chemical Society does have Nuclear Chemistry sections, they are often held in satellite conference spaces. Moving these sections, spatially and intellectually, into the main flow of the conference would represent a small (and symbolic) step in the right direction.

On the flip side, the radiochemistry and nuclear imaging communities can certainly contribute to forging these relationships, too, particularly by seeking out and hiring trained inorganic chemists to develop new ligand frameworks and imaging agents rather than simply relying on commercially available products that have proven “good enough.” In addition, it would behoove the nuclear medicine field to place a greater emphasis on fundamental chemistry, both inorganic and organic, at conferences and symposia and in hospital or university seminar series. Exposure of more biomedically oriented researchers to the cutting edge of pure chemistry can often lead to fruitful and productive collaborations. In the end, the field as a whole will reap the benefits of these strengthened bonds: stronger collaborations, more fluid exchange of ideas, better-trained scientists, and, ultimately, better imaging agents.

In the end, success in addressing these “out of the laboratory” issues will dramatically accelerate scientific progress in both the laboratory and clinic.

Pressing Needs in the Laboratory

Moving into the laboratory, the next five years of science at the intersection of inorganic chemistry and nuclear medicine will be an exciting time. Progress is needed and will surely be made on a wide variety of fronts. Yet we feel it is especially important to briefly discuss three particularly pressing needs, each inspired by a case study discussed above.

1. Drive for New Chelators—The ^{68}Ga-DOTATOC case study illuminated the critical role of chelator choice in the success of an imaging agent. As we have discussed, selecting a chelator for an imaging agent requires a delicate balancing act. The appropriateness of the

chelator for the chosen radiometal must first be considered but so too must the structure of the chelator itself.[4] Macrocyclic chelators typically offer greater stability but often require elevated labeling temperatures, which may compromise sensitive biomolecule vectors; conversely, acyclic chelators often label quickly and easily but are generally slightly less stable in vivo. Thus, it becomes clear that chelators combining the thermodynamic stability and kinetic inertness of macrocyclic chelators with the facile radiolabeling of acyclic chelators could be tremendously valuable tools. The ultimate goal, of course, is an ideal chelator: one that can be labeled quickly and cleanly at room temperature and forms a complex with high kinetic and thermodynamic stabilities.

In this regard, newer generations of chelators have offered dramatic improvements over old workhorses like DOTA and DTPA, first with NOTA, CHX-A″-DTPA, and CB-TE2A and more recently with constructs based on sarcophagine, triazacyclononane-phosphinic acid, and pyridinecarboxylate scaffolds.[29,164,264,265] However, there is still some room for improvement, particularly in the development of chelators that offer *both* mild labeling conditions and high in vivo stability. Further, while the development of radiometal-specific chelators has proven the simplest route, chelators capable of effectively coordinating multiple different radioisotopes are particularly desirable because of their potential use with imaging and therapy isotopic pairs. New ligands for $^{89}Zr^{4+}$ are an especially pressing need because only one (DFO) has proven effective to date. While DFO stably sequesters ^{89}Zr, an octadentate chelator may further increase the stability, thereby eliminating the release of $^{89}Zr^{4+}$ in vivo and preventing the background uptake in bone observed in many preclinical studies (vide supra).

Inorganic chemists and nuclear imaging scientists share a mutual responsibility for the advancement of new chelators. On the chemistry side, it is critical that chemists include in their publications the data most relevant to nuclear medicine, including stability measurements under physiological conditions and comparisons to more established chelators performed under standardized conditions. Further, because in vivo experiments are not feasible in many chemistry departments, it is essential that chemists either make bifunctional variants of their chelators available to the nuclear imaging community or, preferably, develop collaborations with nuclear imaging scientists in order to facilitate in vivo experiments and push their chelators toward the clinic. On the flip side, imaging scientists must seek out new, better chelators rather than simply rely on established ones.

This cooperation is particularly important given the exigencies of clinical regulatory review. The process is invariably slow and expensive and, as a result, possesses an intrinsic inertia. Once an imaging agent has started down this path, there is an understandable resistance to change, even if the current chelator is merely “good enough”. The ^{68}Ga-DOTATOC story provides an excellent example of this phenomenon. This makes the initial choice of a chelator especially critical, and it is up to both inorganic chemists and imaging scientists to work together to make sure that the best choices are made.

2. Developing Radiotracers Based on Small Metal Complexes—As we have seen in the ^{64}Cu-ATSM and ^{99m}Tc-sestamibi case studies, a variety of imaging agents based on small metal complexes, also including ^{99m}Tc-Myoview and ^{99m}Tc-Technecard, have been

developed and effectively translated to the clinic. However, these agents have typically been limited to delineating perfusion or hypoxia.[18,19] Targeting specific molecular biomarkers, on the other hand, has remained the domain of radiolabeled bioconjugates and small organic molecules labeled with radiohalogens. This need not be the case. Metal complexes offer a versatile scaffold for the creation of three-dimensional molecular recognition architectures capable of specifically binding enzymes or antigens. Indeed, while the ability of metal complexes to selectively target DNA has been an area of study for decades, recent years have witnessed a surge of interest in metal complexes as enzyme inhibitors.[266,267] Further, the inherent modularity of metal complexes could facilitate alterations to both the ligand environment and overall charge of the complex in order to optimize the affinity, selectivity, and in vivo pharmacokinetics and pharmacodynamics.

3. Expanding the Repertoire of Biological Events That Can Be Imaged—The ability of ^{89}Zr-Tf to move beyond constituitively expressed cancer biomarkers and provide information about “druggable” cellular pathways underlines the importance of expanding and broadening the array of biological targets for imaging. There is a troubling tendency among preclinical researchers to “overstudy” tumor-targeting strategies for which robust technologies already exist. One prominent example is the prostate-specific membrane antigen, a prostate cancer-associated biomarker for which new technologies are continuously published despite the existence of two fully humanized antibodies (7E11 and J591) and several highly potent and selective small molecules.[268] A far more pressing need for the community is the creation of new approaches to address pathological events that currently cannot be imaged. Listed below are two such examples accompanied by brief explanations as to how a more dedicated chemical effort might bring about rapid advances.

Oligonucleotide Imaging: In essence, cancer is a disease of genomic instability and transcriptional rewiring, and in this regard, the most conceptually obvious manner to distinguish malignant from normal tissue is to exploit these changes.[269] The clinical relevance of radiolabeled antisense oligonucleotides is debated, owing to the generally poor in vivo stability and pharmacokinetics of these molecules. However, antisense nucleotides are not the only molecules capable of selectively and specifically binding nucleic acids.[270] Indeed, the well-established capacity for metal complexes to selectively target certain regions of DNA may be an untapped resource for radiotracer development. Along these lines, the modularity of the ligand environment of metal complexes could be especially advantageous because it could be exploited to customize the selectivity of the complexes for sequence-dependent recognition.

Post-translational Modifications: The aberrant pro-survival and proliferative signaling endemic to cancer also require the stable upregulation of many post-translational modifications to biomolecules, including protein phosphorylation, protein ubiquitination, and DNA methylation.[269] To our knowledge, no groups have successfully developed radiotracers capable of distinguishing any post-translational event. As with oligonucleotides, leveraging the exquisite selectivity and affinity of antibodies to target these motifs is controversial because the ability of technologies like cell-penetrating peptides (e.g., TAT) to deliver antibodies to cytosolic antigens is still subject to debate.[271] In this regard, freely

diffusing small molecules, either metal complexes or organic molecules, would seem to be the most feasible option, and some encouraging progress in selectively targeting post-translational events with small-molecule "cages" has been made within the molecular recognition community.[272] This progress would seem to foreshadow a milestone study for both the imaging and radiotherapy fields, pending a more aggressive effort to optimize these reagents for in vivo applications.

CONCLUSION

In the preceding pages, it was our aim to shed light not only on the critical role that inorganic chemistry has played in the synthesis and development of nuclear imaging agents but also on the power and promise of radiometal-based PET and SPECT probes in the clinic. The case studies clearly illustrate the structural and functional diversity that radiometals make possible. These agents run the structural gamut from discrete metal complexes (^{64}Cu-ATSM) to massive macromolecular assemblies (^{99m}Tc-colloids) and have been used to effectively image targets ranging from myocardial perfusion (^{99m}Tc-sestamibi) to oncogenic biomarkers (^{68}Ga-DOTATOC). Further, while four of the five case studies described probes currently used in the clinic, many more, represented here by ^{89}Zr-Tf, have shown significant preclinical promise and lie on the cusp of translation to the bedside.

Yet our intention here was not simply to celebrate the fruitful intersection of inorganic chemistry and nuclear imaging. We also hope that this discussion spurs renewed enthusiasm in the inorganic chemistry community for radiometals and nuclear imaging because we believe that the work of inorganic chemists will be absolutely indispensible as the field pushes back current frontiers. Ultimately, we sincerely believe that only an interdisciplinary collaboration between inorganic chemists, radiochemists, imaging scientists, and clinicians will be able to fully harness the immense potential of radiometals as diagnostic tools.

References

1. Strauss, HW.; Mariani, G.; Volterrani, D.; Larson, SM. Nuclear Oncology: Pathophysiology and Clinical Applications. Springer; New York: 2012.
2. Heller, GV.; Hendel, RC. Handbook of Nuclear Cardiology: Cardiac SPECT and Cardiac PET. Springer; New York: 2012.
3. Wadas TJ, Wong EH, Weisman GR, Anderson CJ. Curr Pharm Des. 2007; 13:3–16. [PubMed: 17266585]
4. Wadas TJ, Wong EH, Weisman GR, Anderson CJ. Chem Rev. 2010; 110:2858–2902. [PubMed: 20415480]
5. Zeglis BM, Lewis JS. Dalton Trans. 2011; 40:6168–6195. [PubMed: 21442098]
6. Reichert DE, Lewis J, Anderson CJ. Coord Chem Rev. 1999; 184:3–66.
7. Liu S, Edwards DS. Chem Rev. 1999; 99:2235–2268. [PubMed: 11749481]
8. Kelkar SS, Reineke TM. Bioconjugate Chem. 2011; 22:1879–1903.
9. Jagoda EM, Lang L, Bhadrasetty V, Histed S, Williams M, Kramer-Marek G, Mena E, Rosenblum L, Marik J, Tinianow JN, Merchant M, Szajek L, Paik C, Cecchi F, Raffensperger K, Jose-Dizon JM, Bottaro DP, Choyke P. J Nucl Med. 2012; 53:1592–1600. [PubMed: 22917884]
10. Blower PJ, Lewis JS, Zweit J. Nucl Med Biol. 1996; 23:957–980. [PubMed: 9004284]
11. Deri MA, Zeglis BM, Francesconi LC, Lewis JS. Nucl Med Biol. 2012; 40:3–14. [PubMed: 22998840]

12. Sadeghi M, Aboudzadeh M, Zali A, Mirzaii M, Bolourinovin F. Appl Radiat Isot. 2009; 67:7–10. [PubMed: 18930657]
13. Sadeghi M, Aboudzadeh M, Zali A, Zeinali B. Appl Radiat Isot. 2009; 67:1392–1396. [PubMed: 19285420]
14. Yoo J, Tang L, Perkins TA, Rowland DJ, Laforest R, Lewis JS, Welch MJ. Nucl Med Biol. 2005; 32:891–897. [PubMed: 16253815]
15. Holland JP, Sheh YC, Lewis JS. Nucl Med Biol. 2009; 36:729–739. [PubMed: 19720285]
16. Meijs WE, Herscheid JDM, Haisma HJ, Wijbrandts R, Vanlangevelde F, Vanleuffen PJ, Mooy R, Pinedo HM. Appl Radiat Isot. 1994; 45:1143–1147.
17. Brechbiel MW. Q J Nucl Med Mol Imaging. 2008; 52:166–173. [PubMed: 18043537]
18. Mewis RE, Archibald SJ. Coord Chem Rev. 2010; 254:1686–1712.
19. Carroll V, Demoin DW, Hoffman TJ, Jurisson SS. Radiochim Acta. 2012; 100:653–667.
20. Jurisson SS, Lydon JD. Chem Rev. 1999; 99:2205–2218. [PubMed: 11749479]
21. Liu S. Chem Soc Rev. 2004; 33:445–461. [PubMed: 15354226]
22. Anderson CJ, Ferdani R. Cancer Biother Radiopharm. 2009; 24:379–393. [PubMed: 19694573]
23. Bakaj M, Zimmer M. J Mol Struct. 1999; 508:59–72.
24. Shokeen M, Anderson CJ. Acc Chem Res. 2009; 42:832–841. [PubMed: 19530674]
25. Wadas TJ, Anderson CJ. Nat Protoc. 2006; 1:3062–3068. [PubMed: 17406569]
26. Smith SV. J Inorg Biochem. 2004; 98:1874–1901. [PubMed: 15522415]
27. Prasanphanich AF, Nanda PK, Rold TL, Ma LX, Lewis MR, Garrison JC, Hoffman TJ, Sieckman GL, Figueroa SD, Smith CJ. Proc Natl Acad Sci USA. 2007; 104:12462–12467. [PubMed: 17626788]
28. Smith SV. Q J Nucl Med Mol Imaging. 2008; 52:193–202. [PubMed: 18174877]
29. Voss SD, Smith SV, DiBartolo N, McLntos LJ, Cyr EM, Bonab AA, Dearling JLJ, Carter EA, Fischman AJ, Treves ST, Gillies SD, Sargeson AM, Huston JS, Packard AB. Proc Natl Acad Sci USA. 2007; 104:17489–17493. [PubMed: 17954911]
30. Green MA, Welch MJ. Int J Radiat Appl Instrum, Part B. 1989; 16:435–448.
31. Bartholoma MD, Louie AS, Valliant JF, Zubieta J. Chem Rev. 2010; 110:2903–2920. [PubMed: 20415476]
32. Morfin JF, Toth E. Inorg Chem. 2011; 50:10371–10378. [PubMed: 21902283]
33. Bandoli G, Dolmella A, Tisato F, Porchia M, Refosco F. Coord Chem Rev. 2009; 253:56–77.
34. Weiner RE, Thakur ML. Handb Radiopharm. 2003:363–399.
35. Blend MJ, Stastny JJ, Swanson SM, Brechbiel MW. Cancer Biother Radiopharm. 2003; 18:355–363. [PubMed: 12954122]
36. Li YJ, Martell AE, Hancock RD, Reibenspies JH, Anderson CJ, Welch MJ. Inorg Chem. 1996; 35:404–414. [PubMed: 11666222]
37. Ma R, Motekaitis RJ, Martell AE. Inorg Chim Acta. 1994; 224:151–155.
38. Ma R, Murase I, Martell AE. Inorg Chim Acta. 1994; 223:109–119.
39. Fani M, Andre JP, Maecke HR. Contrast Media Mol Imaging. 2008; 3:53–63. [PubMed: 18383455]
40. Martell, AE.; Hancock, RD. Metal Complexes in Aqueous Solutions. Plenum Press; New York: 1996.
41. Viola-Villegas N, Doyle RP. Coord Chem Rev. 2009; 253:1906–1925.
42. Anderson CJ, Welch MJ. Chem Rev. 1999; 99:2219–2234. [PubMed: 11749480]
43. Broan CJ, Cox JPL, Craig AS, Kataky R, Parker D, Harrison A, Randall AM, Ferguson G. J Chem Soc, Perkin Trans 2. 1991; 1:87–99.
44. Motekaitis RJ, Martell AE, Koch SA, Hwang JW, Quarless DA, Welch MJ. Inorg Chem. 1998; 37:5902–5911.
45. Clarke ET, Martell AE. Inorg Chim Acta. 1991; 181:273–280.
46. Clarke ET, Martell AE. Inorg Chim Acta. 1991; 190:37–46.
47. Delgado R, Dasilva JJR. Talanta. 1982; 29:815–822. [PubMed: 18963244]

48. Maecke H, Riesen A, Ritter W. J Nucl Med. 1989; 30:1235–1239. [PubMed: 2738704]
49. Wei L, Zhang X, Gallazzi F, Miao Y, Jin X, Brechbiel MW, Xu H, Clifford T, Welch MJ, Lewis JS, Quinn TP. Nucl Med Biol. 2009; 36:345–354. [PubMed: 19423001]
50. Zhang HW, Chen JH, Waldherr C, Hinni K, Waser B, Reubi JC, Maecke HR. Cancer Res. 2004; 64:6707–6715. [PubMed: 15374988]
51. Kwekkeboom DJ, Kooij PP, Bakker WH, Macke HR, Krenning EP. J Nucl Med. 1999; 40:762–767. [PubMed: 10319747]
52. de Jong M, Bakker WH, Krenning EP, Breeman WA, van der Pluijm ME, Bernard BF, Visser TJ, Jermann E, Behe M, Powell P, Macke HR. Eur J Nucl Med. 1997; 24:368–371. [PubMed: 9096086]
53. Parker D, Pulukkody K, Smith FC, Batsanov A, Howard JAK. J Chem Soc, Dalton Trans. 1994; 5:689–693.
54. Kumar K, Chang CA, Francesconi LC, Dischino DD, Malley MF, Gougoutas JZ, Tweedle MF. Inorg Chem. 1994; 33:3567–3575.
55. Amin S, Marks C, Toomey LM, Churchill MR, Morrow JR. Inorg Chim Acta. 1996; 246:99–107.
56. Clifford T, Boswell CA, Biddlecombe GB, Lewis JS, Brechbiel MW. J Med Chem. 2006; 49:4297–4304. [PubMed: 16821789]
57. Lewis JS, Laforest R, Lewis MR, Anderson CJ. Cancer Biother Radiopharm. 2000; 15:593–604. [PubMed: 11190491]
58. Smith, RM.; Martell, AE. Critical Stability Constants. Plenum Press; New York: 1989.
59. Koudelkova M, Vinsova H, Jedinakova-Krizova V. Czech J Phys. 2003; 53:A769–A775.
60. Rosch F, Herzog H, Stolz B, Brockmann J, Kohle M, Muhlensiepen H, Marbach P, Muller-Gartner HW. Eur J Nucl Med. 1999; 26:358–366. [PubMed: 10199941]
61. Erkberg C, Kallvenius G, Albinsson Y, Brown PL. J Solution Chem. 2004; 33:47–79.
62. Singhal A, Toth LM, Lin JS, Affholter K. J Am Chem Soc. 1996; 117:11529–11534.
63. Lee DB, Roberts M, Bluchel CG, Odell RA. ASAIO J. 2010; 56:550–556. [PubMed: 21245802]
64. Pozhidaeb AI, Porai-Koshits MA, Polynova TN. J Struct Chem. 1974; 15:548–553.
65. Ilyukhin AB, Davidovich RK, Samsonova IN, Telplukhina LV. Crystallogr Rep. 2000; 45:39–43.
66. Bottari E, Anderegg G. Helv Chim Acta. 1967; 50:2349–2355.
67. Meijs WE, Herscheid JDM, Haisma HJ, Pinedo HM. Appl Radiat Isot. 1992; 43:1443–1447.
68. Meijs WE, Haisma HJ, Van der Schors R, Wijbrandts R, Van den Oever K, Klok RP, Pinedo HM, Herscheid JDM. Nucl Med Biol. 1996; 23:439–448. [PubMed: 8832698]
69. Perk LR, Visser GWM, Budde M, Vosjan MJWD, Jurek P, Kiefer GE, van Dongen GAMS. Nat Protoc. 2008; 5:739–743. [PubMed: 20360768]
70. Vosjan M, Perk LR, Visser GWM, Budde M, Jurek P, Kiefer GE, van Dongen G. Nat Protoc. 2010; 5:739–743. [PubMed: 20360768]
71. Holland JP, Divilov V, Bander NH, Smith-Jones PM, Larson SM, Lewis JS. J Nucl Med. 2010; 51:1293–1300. [PubMed: 20660376]
72. Banerjee SR, Maresca KP, Francesconi L, Valliant J, Babich JW, Zubieta J. Nucl Med Biol. 2005; 32:1–20. [PubMed: 15691657]
73. Prakash S, Went MJ, Blower PJ. Nucl Med Biol. 1996; 23:543–9. [PubMed: 8832713]
74. Peacock, RD. The Chemistry of Technetium and Rhenium. Elsevier Publishing Co; New York: 1966.
75. Zolle, I. Technetium-99 radiopharmaceuticals: Preparation and Quality Control in Nuclear Medicine. 1. Springer; New York: 2006.
76. Stern HS, McAfee JG, Subramanian G. J Nucl Med. 1966; 7:665–675. [PubMed: 5921170]
77. Liu S. Adv Drug Delivery Rev. 2008; 60:1347–1370.
78. Abiraj K, Mansi R, Tamma M-L, Forrer F, Cescato R, Reubi JC, Akyel KG, Maecke HR. Chem—Eur J. 2011; 16:2115–2124. [PubMed: 20066690]
79. Meszaros LK, Dose A, Biagini SCG, Blower PJ. Dalton Trans. 2011; 40:6260–6267. [PubMed: 21350776]

80. Boschi A, Bolzati C, Benini E, Malago E, Uccelli L, Duatti A, Piffanelli A, Refosco F, Tisato F. Bioconjugate Chem. 2001; 12:1035–1042.
81. Fernandes C, Kniess T, Gano L, Seifert S, Spies H, Santos I. Nucl Med Biol. 2004; 31:785–793. [PubMed: 15246370]
82. Pietzsch HJ, Tisato F, Refosco F, Leibnitz P, Drews A, Seifert S, Spies H. Inorg Chem. 2001; 40:59–64. [PubMed: 11195389]
83. Alberto R, Schibli R, Abram U, Egli A, Knapp FF, Schubiger PA. Radiochim Acta. 1997; 79:99–103.
84. Alberto R, Schibli R, Egli A, Schubiger AP, Abram U, Kaden TA. J Am Chem Soc. 1998; 120:7987–7988.
85. Garcia R, Paulo A, Santos I. Inorg Chim Acta. 2009; 362:4315–4327.
86. Bowen ML, Lim NC, Ewart CB, Misri R, Ferreira CL, Haefeli U, Adam MJ, Orvig C. Dalton Trans. 2009; 42:9216–9227. [PubMed: 20449199]
87. Mindt TL, Mueller C, Melis M, de Jong M, Schibli R. Bioconjugate Chem. 2008; 19:1689–1695.
88. Taylor AT, Lipowska M, Marzilli LG. J Nucl Med. 2010; 51:391–396. [PubMed: 20150248]
89. Vitor RF, Esteves T, Marques F, Raposinho P, Paulo A, Rodrigues S, Rueff J, Casimiro S, Costa L, Santos I. Cancer Biother Radiopharm. 2009; 24:551–563. [PubMed: 19877885]
90. Moore AL, Bucar D-K, MacGillivray LR, Benny PD. Dalton Trans. 2010; 39:1926–1928. [PubMed: 20148205]
91. Albertini JJ, Lyman GH, Cox C, Yeatman T, Balducci L, Ku NN, Shivers S, Berman C, Wells K, Rapaport D, Shons A, Horton J, Greenberg H, Nicosia S, Clark R, Cantor A, Reintgen DS. J Am Med Assoc. 1996; 276:1818–1822.
92. Krag D, Weaver D, Ashikaga T, Moffat F, Klimberg VS, Shriver C, Feldman S, Kusminsky R, Gadd M, Kuhn J, Harlow S, Beitsch P. N Engl J Med. 1998; 339:941–946. [PubMed: 9753708]
93. Wilhelm AJ, Mijnhout GS, Franssen EJF. Eur J Nucl Med. 1999; 26:S36–S42. [PubMed: 10199931]
94. Dobson EL, Gofman JW, Jones HB, Kelly LS, Walker LA. J Lab Clin Med. 1949; 34:305–312. [PubMed: 18113918]
95. Vavere AL, Lewis JS. Dalton Trans. 2007; 43:4893–4902. [PubMed: 17992274]
96. Holland JP, Lewis JS, Dehdashti F. Q J Nucl Med Mol Imaging. 2009; 53:193–200. [PubMed: 19293767]
97. Wood KA, Wong WL, Saunders MI. Nucl Med Biol. 2008; 35:393–400. [PubMed: 18482676]
98. Tatum JL, Kelloff GJ, Gillies RJ, Arbeit JM, Brown JM, Chao KSC, Chapman JD, Eckelman WC, Fyles AW, Giaccia AJ, Hill RP, Koch CJ, Krishna MC, Krohn KA, Lewis JS, Mason RP, Melillo G, Padhani AR, Powis G, Rajendran JG, Reba R, Robinson SP, Semenza GL, Swartz HM, Vaupel P, Yang D, Croft B, Hoffman J, Liu G, Stone H, Sullivan D. Int J Radiat Biol. 2006; 82:699–757. [PubMed: 17118889]
99. Graeber TG, Osmanian C, Jacks T, Housman DE, Koch CJ, Lowe SW, Giaccia AJ. Nature. 1996; 379:88–91. [PubMed: 8538748]
100. Hockel M, Schlenger K, Aral B, Mitze M, Schaffer U, Vaupel P. Cancer Res. 1996; 56:4509–4515. [PubMed: 8813149]
101. Fujibayashi Y, Taniuchi H, Yonekura Y, Ohtani H, Konishi J, Yokoyama A. J Nucl Med. 1997; 38:1155–1160. [PubMed: 9225812]
102. Dearling JLJ, Lewis JS, Mullen GED, Rae MT, Zweit J, Blower PJ. Eur J Nucl Med. 1998; 25:788–792. [PubMed: 9662602]
103. Dearling JLJ, Lewis JS, Muller GED, Welch MJ, Blower PJ. J Biol Inorg Chem. 2002; 7:249–259. [PubMed: 11935349]
104. Lewis JS, McCarthy DW, McCarthy TJ, Fujibayashi Y, Welch MJ. J Nucl Med. 1999; 40:177–183. [PubMed: 9935074]
105. Yuan H, Schroeder T, Bowsher JE, Hedlund LW, Wong T, Dewhirst MW. J Nucl Med. 2006; 47:989–998. [PubMed: 16741309]

106. O'Donoghue JA, Zanzonico P, Pugachev A, Wen BX, Smith-Jones P, Cai SD, Burnazi E, Finn RD, Burgman P, Ruan S, Lewis JS, Welch MJ, Ling CC, Humm JL. Int J Radiat Oncol. 2005; 61:1493–1502.

107. Hansen AE, Kristensen AT, Jorgensen JT, McEvoy FJ, Busk M, van der Kogel AJ, Bussink J, Engelholm SA, Kjaer A. Radiat Oncol. 2012; 7:89–97. [PubMed: 22704363]

108. Dence CS, Ponde DE, Welch MJ, Lewis JS. Nucl Med Biol. 2008; 35:713–720. [PubMed: 18678357]

109. Burgman P, O'Donoghue JA, Lewis JS, Welch MJ, Humm JL, Ling CC. Nucl Med Biol. 2005; 32:623–630. [PubMed: 16026709]

110. Matsumoto KI, Szajek L, Krishna MC, Cook JA, Seidel J, Grimes K, Carson J, Sowers AL, English S, Green MV, Bacharach SL, Eckelman WC, Mitchell JB. Int J Oncol. 2007; 30:873–881. [PubMed: 17332926]

111. McCall KC, Humm JL, Bartlett R, Reese M, Carlin S. Int J Radiat Oncol. 2012; 84:E393–E399.

112. Carlin S, Humm JL. J Nucl Med. 2012; 53:1171–1174. [PubMed: 22789676]

113. Dearling JLJ, Packard AB. Nucl Med Biol. 2010; 37:237–243. [PubMed: 20346863]

114. Obata A, Yoshimi E, Waki A, Lewis JS, Oyama N, Welch MJ, Saji H, Yonekura Y, Fujibayashi Y. Ann Nucl Med. 2001; 15:499–504. [PubMed: 11831397]

115. Dearling JLJ, Lewis JS, McCarthy DW, Welch MJ, Blower PJ. Chem Commun. 1998; 22:2531–2532.

116. Maurer RI, Blower PJ, Dilworth JR, Reynolds CA, Zheng YF, Mullen GED. J Med Chem. 2002; 45:1420–1431. [PubMed: 11906283]

117. Castle TC, Maurer RI, Sowrey FE, Went MJ, Reynolds CA, McInnes EJL, Blower PJ. J Am Chem Soc. 2003; 125:10040–10049. [PubMed: 12914467]

118. Blower PJ, Dilworth JR, Maurer RI, Mullen GD, Reynolds CA, Zheng YF. J Inorg Biochem. 2001; 85:15–22. [PubMed: 11377691]

119. Holland JP, Green JC, Dilworth JR. Dalton Trans. 2006; 6:783–794. [PubMed: 16437173]

120. Holland JP, Barnard PJ, Collison D, Dilworth JR, Edge R, Green JC, McInnes EJL. Chem—Eur J. 2008; 14:5890–5907. [PubMed: 18494010]

121. Cowley AR, Dilworth JR, Donnelly PS, Labisbal E, Sousa A. J Am Chem Soc. 2002; 124:5270–5271. [PubMed: 11996559]

122. Harris ED. Nutr Rev. 2001; 59:281–285. [PubMed: 11570430]

123. Liu J, Hajibeigi A, Ren G, Lin M, Siyambalapitiyage W, Liu ZS, Simpson E, Parkey RW, Sun XK, Oz OK. J Nucl Med. 2009; 50:1332–1339. [PubMed: 19617332]

124. Takahashi N, Fujibayashi Y, Yonekura Y, Welch MJ, Waki A, Tsuchida T, Sadato N, Sugimoto K, Itoh H. Ann Nucl Med. 2000; 14:323–328. [PubMed: 11108159]

125. Takahashi N, Fujibayashi Y, Yonekura Y, Welch MJ, Waki A, Tsuchida T, Sadato N, Sugimoto K, Nakano A, Lee JD, Itoh H. Ann Nucl Med. 2001; 15:293–296. [PubMed: 11545205]

126. Dehdashti F, Grigsby PW, Lewis JS, Laforest R, Siegel BA, Welch MJ. J Nucl Med. 2008; 49:201–205. [PubMed: 18199612]

127. Dehdashti F, Grigsby PW, Mintun MA, Lewis JS, Siegel BA, Welch MJ. Int J Radiat Oncol. 2003; 55:1233–1238.

128. Dehdashti F, Mintun MA, Lewis JS, Bradley J, Govindan R, Laforest R, Welch MJ, Siegel BA. Eur J Nucl Med Mol Imaging. 2003; 30:844–850. [PubMed: 12692685]

129. Dietz D, Malyapa R, Myerson R, Grigsby P, Tan B, Ritter J, Welch M, Siegel B, Picus J, Dehdashti F. Dis Colon Rectum. 2007; 50:780–780.

130. Lewis JS, Laforest R, Dehdashti F, Grigsby PW, Welch MJ, Siegel BA. J Nucl Med. 2008; 49:1177–1182. [PubMed: 18552145]

131. Zhang H, Moroz MA, Serganova I, Ku T, Huang R, Vider J, Maecke HR, Larson SM, Blasberg R, Smith-Jones PM. J Nucl Med. 2011; 52:123–131. [PubMed: 21149478]

132. Harris AG. Gut. 1994; 35:1–4. [PubMed: 8307427]

133. Colao A, Faggiano A, Pivonello R. Prog Brain Res. 2010; 182:281–294. [PubMed: 20541670]

134. Bonfils S. Gut. 1985; 26:433–437. [PubMed: 2860051]

135. Krentz AJ, Boyle PJ, Macdonald LM, Schade DS. Metabolism. 1994; 43:24–31. [PubMed: 8289671]
136. Weckbecker G, Raulf F, Stolz B, Bruns C. Clin Pharm Therap. 1993; 60:245–264.
137. Nisa L, Savelli G, Giubbini R. Ann Nucl Med. 2011; 25:75–85. [PubMed: 21107762]
138. Bernard BF, Krenning EP, Breeman WA, Rolleman EJ, Bakker WH, Visser TJ, Macke H, de Jong M. J Nucl Med. 1997; 38:1929–1933. [PubMed: 9430472]
139. Otte A, Jermann E, Behe M, Goetze M, Bucher HC, Roser HW, Heppeler A, Mueller-Brand J, Maecke HR. Eur J Nucl Med. 1997; 24:792–795. [PubMed: 9211767]
140. Chanson P, Timsit J, Harris AG. Clin Pharmacokinet. 1993; 25:375–391. [PubMed: 8287633]
141. Inoue T, Ootake H, Hirano T, Tomiyoshi K, Endo K, Tanaka K, Shimizu N, Saito T. Kaku Igaku. 1995; 32:511–521. [PubMed: 7596072]
142. Barbanoj M, Antonijoan R, Morte A, Grinyo JM, Sola R, Valles J, Peraire C, Cordero JA, Munoz A, Jane F, Obach R. Clin Pharm Therap. 1999; 66:485–491.
143. Viola NA, Rarig RS, Ouellette W, Doyle RP. Polyhedron. 2006; 25:3457–3462.
144. Kubicek V, Havlickova J, Kotek J, Tircso G, Hermann P, Toth E, Lukes I. Inorg Chem. 2010; 49:10960–10969. [PubMed: 21047078]
145. Loc'h C, Maziere B, Comar D. J Nucl Med. 1980; 21:171–173. [PubMed: 6965408]
146. Yano Y, Anger HO. J Nucl Med. 1964; 5:484–487. [PubMed: 14191416]
147. Velikyan I, Maecke H, Langstrom B. Bioconjugate Chem. 2008; 19:569–573.
148. Zhernosekov KP, Filosofov DV, Baum RP, Aschoff P, Bihl H, Razbash AA, Jahn M, Jennewein M, Rosch F. J Nucl Med. 2007; 48:1741–1748. [PubMed: 17873136]
149. Henze M, Schuhmacher J, Hipp P, Kowalski J, Becker DW, Doll J, Macke HR, Hofmann M, Debus J, Haberkorn U. J Nucl Med. 2001; 42:1053–1056. [PubMed: 11438627]
150. Velikyan I, Beyer GJ, Langstrom B. Bioconjugate Chem. 2004; 15:554–560.
151. Velikyan I, Sundberg AL, Lindhe O, Hoglund AU, Eriksson O, Werner E, Carlsson J, Bergstrom M, Langstrom B, Tolmachev V. J Nucl Med. 2005; 46:1881–1888. [PubMed: 16269603]
152. Velikyan I, Xu H, Nair M, Hall H. Nucl Med Biol. 2012; 39:628–639. [PubMed: 22336375]
153. Al-Nahhas A, Win Z, Szyszko T, Singh A, Nanni C, Fanti S, Rubello D. Anticancer Res. 2007; 27:4087–4094. [PubMed: 18225576]
154. Antunes P, Ginj P, Zhang H, Waser B, Baum RP, Reubi JC, Maecke H. Eur J Nucl Med Mol Imaging. 2007; 34:982–993. [PubMed: 17225119]
155. Gabriel M, Decristoforo C, Kendler D, Dobrozemsky G, Heute D, Uprimny C, Kovacs P, Von Guggenberg E, Bale R, Virgolini IJ. J Nucl Med. 2007; 48:508–518. [PubMed: 17401086]
156. Buchmann I, Henze M, Engelbrecht S, Eisenhut M, Runz A, Schaefer M, Schilling T, Haufe S, Herrmann T, Haberkorn U. Eur J Nucl Med Mol Imaging. 2007; 34:1617–1626. [PubMed: 17520251]
157. Koukouraki S, Strauss LG, Georgoulias V, Eisenhut M, Haberkorn U, Dimitrakopoulou-Strauss A. Eur J Nucl Med Mol Imaging. 2006; 33:1115–1122. [PubMed: 16763820]
158. Harris WR, Pecoraro VL. Biochemistry. 1983; 22:292–299. [PubMed: 6402006]
159. Jyo A, Kohno T, Terazono Y, Kawano S. Anal Sci. 1990; 6:323–324.
160. Boros E, Ferreira CL, Patrick BO, Adam MJ, Orvig C. Nucl Med Biol. 2011; 38:1165–1174. [PubMed: 21831655]
161. Simecek J, Schulz M, Notni J, Plutnar J, Kubicek V, Havlickova J, Hermann P. Inorg Chem. 2012; 51:577–590. [PubMed: 22221285]
162. Wangler C, Wangler B, Lehner S, Elsner A, Todica A, Bartenstein P, Hacker M, Schirrmacher R. J Nucl Med. 2011; 52:586–591. [PubMed: 21421712]
163. Eisenwiener KP, Prata MIM, Buschmann I, Zhang HW, Santos AC, Wenger S, Reubi JC, Macke HR. Bioconjugate Chem. 2002; 13:530–541.
164. Notni J, Simecek J, Hermann P, Wester HJ. Chem—Eur J. 2011; 17:14718–14722. [PubMed: 22147338]
165. Notni J, Pohle K, Wester HJ. Eur J Nucl Med Mol Imaging. 2012; 2:28–32.

166. Notni J, Hermann P, Havlickova J, Kotek J, Kubicek V, Plutnar J, Loktionova N, Riss PJ, Rosch F, Lukes I. Chemistry. 2010; 16:7174–7185. [PubMed: 20461824]
167. Berry DJ, Ma Y, Ballinger JR, Tavare R, Koers A, Sunassee K, Zhou T, Nawaz S, Mullen GE, Hider RC, Blower PJ. Chem Commun. 2011; 47:7068–7070.
168. Andre JP, Maecke HR, Zehnder M, Macko L, Akyel KG. Chem Commun. 1998:1301–1302.
169. Lin M, Welch MJ, Lapi SE. Mol Imaging Biol. 2013; 15:606–613. [PubMed: 23529373]
170. Richardson DR. Adv Exp Med Biol. 2002; 509:231–249. [PubMed: 12572997]
171. Taetle R, Honeysett JM, Trowbridge I. Int J Cancer. 1983; 32:343–349. [PubMed: 6309680]
172. Qian ZM, Li H, Sun H, Ho K. Pharmacol Rev. 2002; 54:561–587. [PubMed: 12429868]
173. Smith TA, Walton PH. Nucl Med Commun. 2002; 23:1085–1090. [PubMed: 12411837]
174. Larson SM. Semin Nucl Med. 1978; 8:193–203. [PubMed: 213849]
175. Front D, Bar-Shalom R, Israel O. Semin Nucl Med. 1997; 27:68–74. [PubMed: 9122725]
176. Edwards CL, Hayes RL. J Nucl Med. 1969; 10:103–105. [PubMed: 5784705]
177. Lee SI, Kim EM, Kim SL, Lee CM, Jang KY, Yun HJ, Yoo WH, Sohn MH, Jeong HJ. Rheumatol Int. 2008; 29:153–157. [PubMed: 18696076]
178. Colonna P, Rain JD, Pecking A, Briere J, Najean Y. Nouv Rev Fr Hematol. 1978; 20:455–464. [PubMed: 754176]
179. James AE Jr, Strauss HW, Fischer K, Wheeless CR, Longo R. Obstet Gynecol. 1971; 37:602–611. [PubMed: 5547858]
180. Arrago JP, Rain JD, Vigneron N, Poirier O, Chomienne C, D'Agay MF, Najean Y. Am J Hematol. 1985; 18:275–282. [PubMed: 3976644]
181. Smith FA, Lurie DJ, Brady F, Danpure HJ, Kensett MJ, Osman S, Silvester DJ, Waters SL. Int J Appl Radiat Isot. 1984; 35:501–506. [PubMed: 6735495]
182. Som P, Oster ZH, Matsui K, Guglielmi G, Persson BR, Pellettieri ML, Srivastava SC, Richards P, Atkins HL, Brill AB. Eur J Nucl Med. 1983; 8:491–494. [PubMed: 6653610]
183. Kumar V, Boddeti DK, Evans SG, Roesch F, Howman-Giles R. Nucl Med Biol. 2011; 38:393–398. [PubMed: 21492788]
184. Otsuki H, Brunetti A, Owens ES, Finn RD, Blasberg RG. J Nucl Med. 1989; 30:1676–1685. [PubMed: 2795208]
185. de Kaski MC, Peters AM, Bradley D, Hodgson HJ. Eur J Nucl Med. 1996; 23:530–533. [PubMed: 8698057]
186. Berry CR, Fisher P, Koblik PD, Guilford WG, Hornof WH. Am J Vet Res. 1997; 58:1188–1192. [PubMed: 9361875]
187. Mintun MA, Dennis DR, Welch MJ, Mathias CJ, Schuster DP. J Nucl Med. 1987; 28:1704–1716. [PubMed: 3499492]
188. Kaplan JD, Calandrino FS, Schuster DP. Am Rev Respir Dis. 1991; 143:150–154. [PubMed: 1986672]
189. Nakamura K, Kawaguchi H, Orii H. Radioisotopes. 1983; 32:163–166. [PubMed: 6635261]
190. Weiner R. Int J Radiat Appl Instrum, Part B. 1990; 17:141–149.
191. Berry CR, Guilford WG, Koblik PD, Hornof WH, Fisher P. Vet Radiol Ultrasound. 1997; 38:221–225. [PubMed: 9238794]
192. Li H, Sadler PJ, Sun H. Eur J Biochem. 1996; 242:387–393. [PubMed: 8973657]
193. Sun H, Cox MC, Li H, Mason AB, Woodworth RC, Sadler PJ. FEBS Lett. 1998; 422:315–320. [PubMed: 9498807]
194. Weiner RE. J Nucl Med. 1989; 30:70–79. [PubMed: 2536083]
195. Bruehlmeier M, Leenders KL, Vontobel P, Calonder C, Antonini A, Weindl A. J Nucl Med. 2000; 41:781–787. [PubMed: 10809192]
196. Vavere AL, Welch MJ. J Nucl Med. 2005; 46:683–690. [PubMed: 15809492]
197. Roelcke U, Leenders KL, von Ammon K, Radu EW, Vontobel P, Gunther I, Psylla M. J Neuro-Oncol. 1996; 29:157–165.
198. Tinoco AD, Valentine AM. J Am Chem Soc. 2005; 127:11218–11219. [PubMed: 16089431]

199. Guo M, Sun H, McArdle HJ, Gambling L, Sadler PJ. Biochemistry. 2000; 39:10023–10033. [PubMed: 10955990]
200. Borjesson PK, Jauw YW, Boellaard R, de Bree R, Comans EF, Roos JC, Castelijns JA, Vosjan MJ, Kummer JA, Leemans CR, Lammertsma AA, van Dongen GA. Cancer Res. 2006; 12:2133–2140.
201. Verel I, Visser GW, Boerman OC, van Eerd JE, Finn R, Boellaard R, Vosjan MJ, Stigter-van Walsum M, Snow GB, van Dongen GA. Cancer Biother Radiopharm. 2003; 18:655–661. [PubMed: 14503961]
202. Wu AM, Olafsen T. Cancer J. 2008; 14:191–197. [PubMed: 18536559]
203. Aloj L, Jogoda E, Lang L, Caraco C, Neumann RD, Sung C, Eckelman WC. J Nucl Med. 1999; 40:1547–1555. [PubMed: 10492378]
204. Prost AC, Anakok M, Aurengo A, Salomon JC, Legrand JC, Rosselin G. Int J Radiat Appl Instrum, Part B. 1990; 17:209–216.
205. Aloj L, Lang L, Jagoda E, Neumann RD, Eckelman WC. J Nucl Med. 1996; 37:1408–1412. [PubMed: 8708785]
206. Zhou Y, Baidoo KE, Brechbiel MW. Adv Drug Delivery Rev. 2012; 65:1098–1111.
207. Jin H, Yang R, Zheng Z, Romero M, Ross J, Bou-Reslan H, Carano RA, Kasman I, Mai E, Young J, Zha J, Zhang Z, Ross S, Schwall R, Colbern G, Merchant M. Cancer Res. 2008; 68:4360–4368. [PubMed: 18519697]
208. Holland JP, Williamson MJ, Lewis JS. Mol Imaging. 2010; 9:1–20. [PubMed: 20128994]
209. Vugts DJ, Visser GW, van Dongen GA. Curr Med Chem. 2013; 13:446–457.
210. Severin GW, Engle JW, Barnhart TE, Nickles RJ. Med Chem. 2011; 7:389–394. [PubMed: 21711221]
211. Holland JP, Caldas-Lopes E, Divilov V, Longo VA, Taldone T, Zatorska D, Chiosis G, Lewis JS. PLoS ONE. 2010; 5:e8859. [PubMed: 20111600]
212. Borjesson PKE, Jauw YWS, de Bree R, Roos JC, Castelijns JA, Leemans CR, van Dongen G, Boellaard R. J Nucl Med. 2009; 50:1828–1836. [PubMed: 19837762]
213. Perk LR, Visser GWM, Vosjan M, Stigter-van Walsum M, Tijink BM, Leemans CR, van Dongen G. J Nucl Med. 2005; 46:1898–1906. [PubMed: 16269605]
214. Nagengast WB, de Korte MA, Munnink THO, Timmer-Bosscha H, den Dunnen WF, Hollema H, de Jong JR, Jensen MR, Quadt C, Garcia-Echeverria C, van Dongen GAMS, Lub-de Hooge MN, Schroder CP, de Vries EGE. J Nucl Med. 2010; 51:761–767. [PubMed: 20395337]
215. Munnink THO, de Korte MA, Nagengast WB, Timmer-Bosscha H, Schroder CP, de Jong JR, van Dongen G, Jensen MR, Quadt C, Lub-de Hooge MN, de Vries EGE. Eur J Cancer. 2010; 46:678–684. [PubMed: 20036116]
216. Heskamp S, van Laarhoven HW, Molkenboer-Kuenen JD, Franssen GM, Versleijen-Jonkers YM, Oyen WJ, van der Graaf WT, Boerman OC. J Nucl Med. 2010; 51:1565–1572. [PubMed: 20847162]
217. Ulmert D, Evans MJ, Holland JP, Rice SL, Wongvipat J, Pettersson K, Abrahamsson PA, Scardino PT, Larson SM, Lilja H, Lewis JS, Sawyers CL. Cancer Discovery. 2012; 2:320–327. [PubMed: 22576209]
218. Hoeben BAW, Kaanders J, Franssen GM, Troost EGC, Rijken P, Oosterwijk E, van Dongen G, Oyen WJG, Boerman OC, Bussink J. J Nucl Med. 2010; 51:1076–1083. [PubMed: 20554724]
219. Evans MJ, Holland JP, Rice SL, Doran MG, Cheal SM, Campos C, Carlin SD, Mellinghoff IK, Sawyers CL, Lewis JS. J Nucl Med. 2013; 54:90–95. [PubMed: 23236019]
220. Zhong W, Parkinson JA, Guo M, Sadler PJ. J Biol Inorg Chem. 2002; 7:589–599. [PubMed: 12072964]
221. O'Donnell KA, Yu D, Zeller KI, Kim JW, Racke F, Thomas-Tikhonenko A, Dang CV. Mol Cell Biol. 2006; 26:2373–2386. [PubMed: 16508012]
222. Marazzi L, Parodi MT, Di Martino D, Ferrari S, Tonini GP. Anticancer Res. 1991; 11:947–952. [PubMed: 2064352]
223. Okazaki F, Matsunaga N, Okazaki H, Utoguchi N, Suzuki R, Maruyama K, Koyanagi S, Ohdo S. Cancer Res. 2010; 70:6238–6246. [PubMed: 20631077]

224. Tacchini L, Bianchi L, Bernelli-Zazzera A, Cairo G. J Biol Chem. 1999; 274:24142–24146. [PubMed: 10446187]
225. Bayeva M, Khechaduri A, Puig S, Chang HC, Patial S, Blackshear PJ, Ardehali H. Cell Metabolism. 2012; 16:645–657. [PubMed: 23102618]
226. Galvez T, Teruel MN, Heo WD, Jones JT, Kim ML, Liou J, Myers JW, Meyer T. Genome Biol. 2007; 8:R142. [PubMed: 17640392]
227. Cao H, Chen J, Krueger EW, McNiven MA. Mol Cell Biol. 2010; 30:781–792. [PubMed: 19995918]
228. Jian J, Yang Q, Huang X. J Biol Chem. 2011; 286:35708–35715. [PubMed: 21859709]
229. Watson PA, Ellwood-Yen K, King JC, Wongvipat J, Lebeau MM, Sawyers CL. Cancer Res. 2005; 65:11565–11571. [PubMed: 16357166]
230. Ellwood-Yen K, Graeber TG, Wongvipat J, Iruela-Arispe ML, Zhang J, Matusik R, Thomas GV, Sawyers CL. Cancer Cell. 2003; 4:223–238. [PubMed: 14522256]
231. Holland JP, Evans MJ, Rice SL, Wongvipat J, Sawyers CL, Lewis JS. Nat Med. 2012; 18:1586–1591. [PubMed: 23001181]
232. Gurel B, Iwata T, Koh CM, Jenkins RB, Lan F, Van Dang C, Hicks JL, Morgan J, Cornish TC, Sutcliffe S, Isaacs WB, Luo J, De Marzo AM. Mod Pathol. 2008; 21:1156–1167. [PubMed: 18567993]
233. Jenkins RB, Qian J, Lieber MM, Bostwick DG. Cancer Res. 1997; 57:524–531. [PubMed: 9012485]
234. Banerjee S, Pillai MR, Ramamoorthy N. Semin Nucl Med. 2001; 31:260–277. [PubMed: 11710769]
235. Jain D. Semin Nucl Med. 1999; 29:221–236. [PubMed: 10433338]
236. Seaborg G, Segre E. Phys Rev. 1939; 55:808–814.
237. Richards P, Tucker WD, Srivastava SC. Int J Appl Radiat Isot. 1982; 33:793–799. [PubMed: 6759417]
238. Boyd RE. Int J Appl Radiat Isot. 1982; 33:801–809. [PubMed: 7152707]
239. Holman BL, Jones AG, Lister-James J, Davison A, Abrams MJ, Kirshenbaum JM, Tumeh SS, English RJ. J Nucl Med. 1984; 25:1350–1355. [PubMed: 6334145]
240. Crane P, Laliberte R, Heminway S, Thoolen M, Orlandi C. Eur J Nucl Med. 1993; 20:20–25. [PubMed: 7678396]
241. Wackers FJ, Berman DS, Maddahi J, Watson DD, Beller GA, Strauss HW, Boucher CA, Picard M, Holman BL, Fridrich R, et al. J Nucl Med. 1989; 30:301–311. [PubMed: 2525610]
242. Marcassa C, Marzullo P, Parodi O, Sambuceti G, L'Abbate A. J Nucl Med. 1990; 31:173–177. [PubMed: 2313356]
243. Borges-Neto S, Coleman RE, Jones RH. J Nucl Med. 1990; 31:1128–1132. [PubMed: 2362191]
244. Mansour S, Roy D, Bouchard V, Nguyen B, Stevens L, Gobeil F, Rivard A, Leclerc G, Reeves F, Noiseux N. J Cardio Trans Res. 2010; 3:153–159.
245. Prats E, Aisa F, Abos MD, Villavieja L, Garcia-Lopez F, Asenjo MJ, Razola P, Banzo J. J Nucl Med. 1999; 40:296–301. [PubMed: 10025838]
246. Imbriaco M, Del Vecchio S, Riccardi A, Pace L, Di Salle F, Di Gennaro F, Salvatore M, Sodano A. Eur J Nucl Med. 2001; 28:56–63. [PubMed: 11202453]
247. Palmedo H, Biersack HJ, Lastoria S, Maublant J, Prats E, Stegner HE, Bourgeois P, Hustinx R, Hilson AJ, Bischof-Delaloye A. Eur J Nucl Med. 1998; 25:375–385. [PubMed: 9553167]
248. Waxman AD. Semin Nucl Med. 1997; 27:40–54. [PubMed: 9122723]
249. Hendrikse NH, Franssen EJ, van der Graaf WT, Vaalburg W, de Vries EG. Eur J Nucl Med. 1999; 26:283–293. [PubMed: 10079321]
250. Van de Wiele C, Rottey S, Geothals I, Buscombe J, Van Belle S, De Vos F, Dierckx R. Nucl Med Commun. 2003; 24:945–950. [PubMed: 12960592]
251. Coakley AJ. Eur J Nucl Med. 1991; 18:151–152. [PubMed: 2040336]
252. Wei JP, Burke GJ, Mansberger AR Jr. Surgery. 1992; 112:1111–1116. [PubMed: 1455313]

253. McBiles M, Lambert AT, Cote MG, Kim SY. Semin Nucl Med. 1995; 25:221–234. [PubMed: 7570042]
254. Alberto R, Schibli R, Schubiger AP, Abram U, Pietzsch HJ, Johannsen B. J Am Chem Soc. 1999; 121:6076–6077.
255. Mindt TL, Muller C, Stuker F, Salazar JF, Hohn A, Mueggler T, Rudin M, Schibli R. Bioconjugate Chem. 2009; 20:1940–1949.
256. Jurisson S, Cutler C, Smith SV. Q J Nucl Med Mol Imaging. 2008; 52:222–234. [PubMed: 18480740]
257. Bergqvist L, Strand SE, Persson BR. Semin Nucl Med. 1983; 13:9–19. [PubMed: 6220471]
258. Lin MS, Winchell HS. J Nucl Med. 1972; 13:58–65. [PubMed: 4621447]
259. Tsopelas C. Q J Nucl Med Mol Imaging. 2005; 49:319–324. [PubMed: 16407815]
260. Whateley TL, Steele G. Eur J Nucl Med. 1985; 10:353–357. [PubMed: 4006978]
261. Cox CE, Pendas S, Cox JM, Joseph E, Shons AR, Yeatman T, Ku NN, Lyman GH, Berman C, Haddad F, Reintgen DS. Ann Surg. 1998; 227:645–651. [PubMed: 9605656]
262. Alazraki NP, Eshima D, Eshima LA, Herda SC, Murray DR, Vansant JP, Taylor AT. Semin Nucl Med. 1997; 27:55–67. [PubMed: 9122724]
263. Pandit-Taskar N, Dauer LT, Montgomery L, StGermain J, Zanzonico PB, Divgi CR. J Nucl Med. 2006; 47:1202–1208. [PubMed: 16818956]
264. Boros E, Ferreira CL, Cawthray JF, Price EW, Patrick BO, Wester DW, Adam MJ, Orvig C. J Am Chem Soc. 2010; 132:15726–15733. [PubMed: 20958034]
265. Price EW, Cawthray JF, Bailey GA, Ferreira CL, Boros E, Adam MJ, Orvig C. J Am Chem Soc. 2012; 134:8670–8683. [PubMed: 22540281]
266. Kilpin KJ, Dyson PJ. Chem Sci. 2013; 4:1410–1419.
267. Che C-M, Siu F-M. Curr Opin Chem Biol. 2012; 14:255–261. [PubMed: 20018553]
268. Mease RC, Foss CA, Pomper MG. Curr Med Chem. 2013; 13:951–962.
269. Hanahan D, Weinberg RA. Cell. 2000; 100:57–70. [PubMed: 10647931]
270. Zeglis BM, Pierre VC, Barton JK. Chem Commun. 2007; 44:4565–4579.
271. Marschall AL, Frenzel A, Schirrmann T, Schungel M, Dubel S. mAbs. 2011; 3:3–16. [PubMed: 21099369]
272. Hargrove AE, Nieto S, Zhang T, Sessler JL, Anslyn EV. Chem Rev. 2011; 111:6603–6782. [PubMed: 21910402]

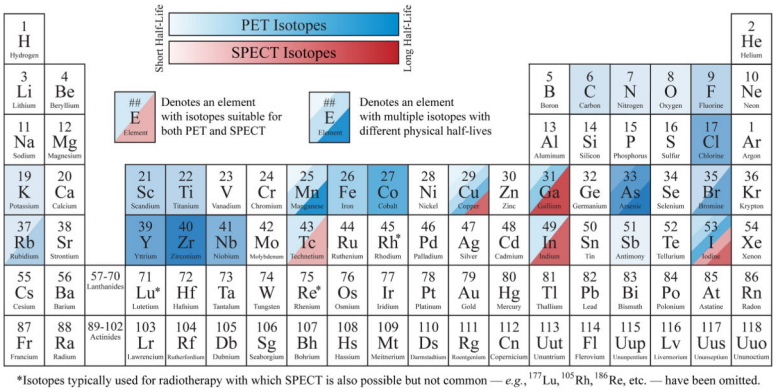

Figure 1.

Illustration of the variety of metals with isotopes suitable for nuclear imaging. Elements with isotopes suitable for PET are color-coded blue, and elements with isotopes suitable for SPECT are color-coded red. The shading corresponds to half-life, with longer half-lives darker and shorter half-lives lighter. Elements with multiple shadings have multiple isotopes suitable for imaging.

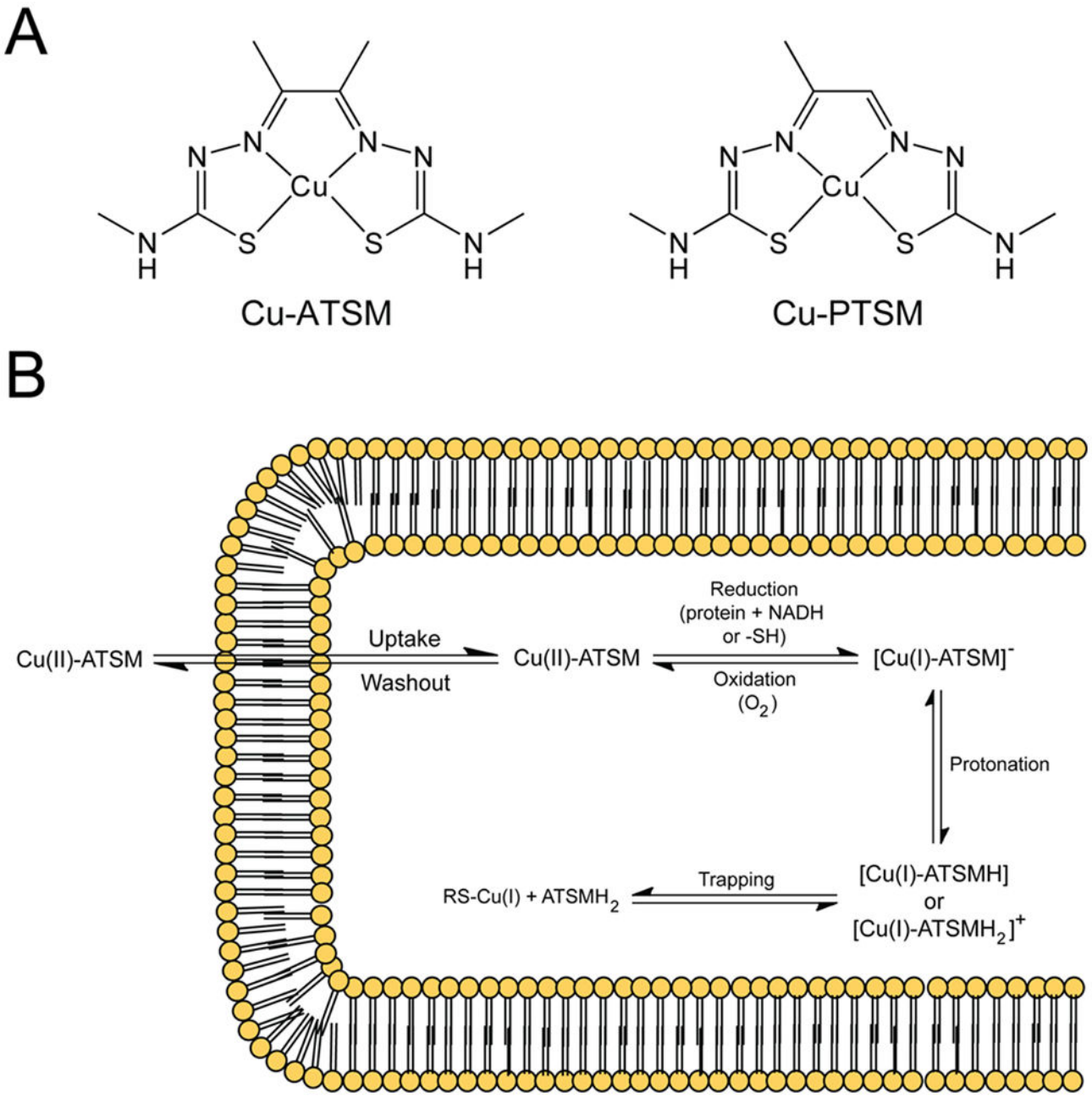

Figure 2.

(A) Structures of hypoxia-selective Cu-ATSM and nonselective Cu-PTSM. (B) Possible mechanistic scheme for the uptake and retention of Cu-ATSM in hypoxic cells.

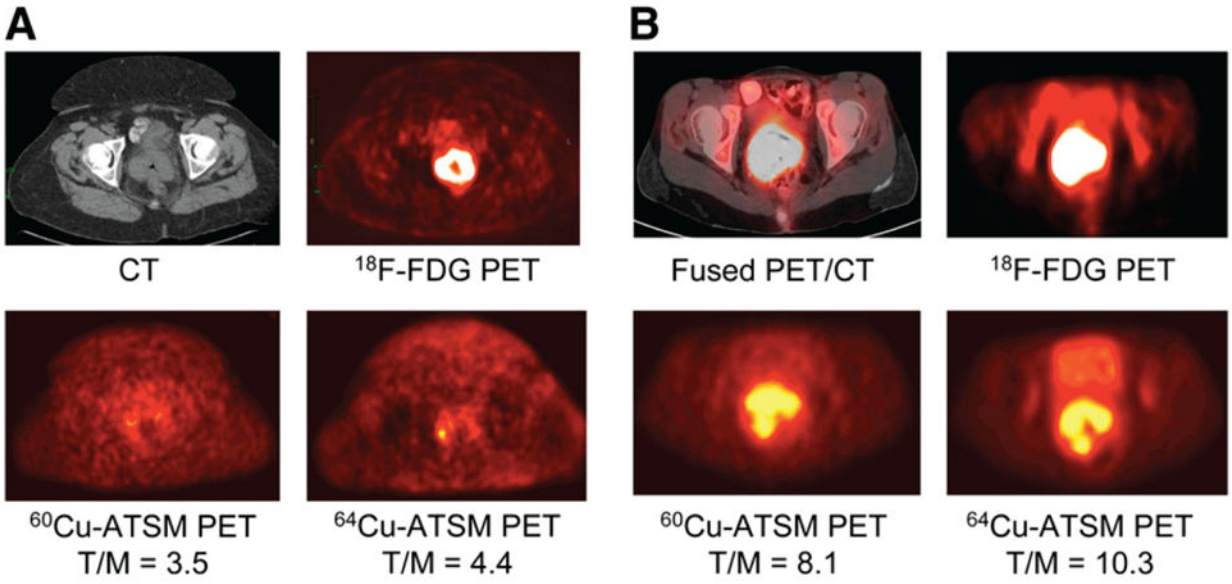

Figure 3.

Transaxial CT (top left), ^{18}F-FDG PET (top right), ^{60}Cu-ATSM PET (bottom left), and ^{64}Cu-ATSM PET (bottom right) of two patients with cancer of the uterine cervix. Panel A displays the images from a patient who responded to therapy, whereas panel B displays the images of a nonresponder. This research was originally published in the *Journal of Nuclear Medicine* (see ref 130). Copyright 2008 Society of Nuclear Medicine and Molecular Imaging, Inc.

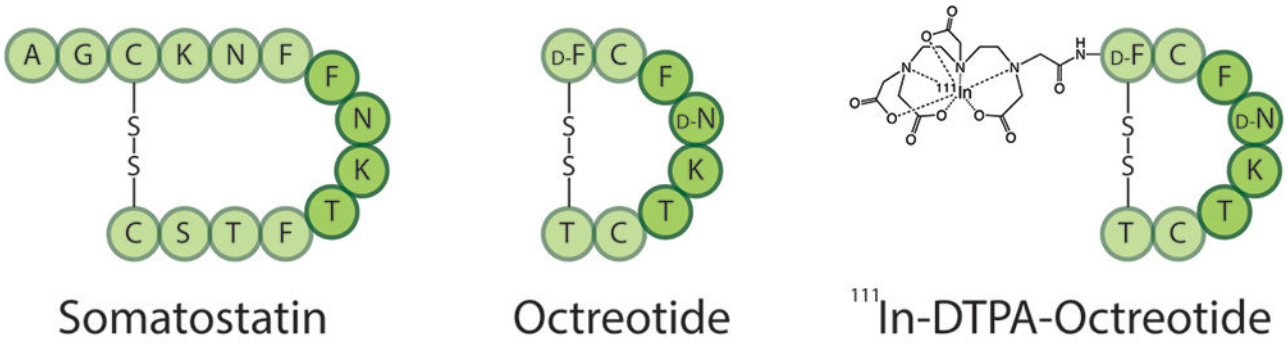

Figure 4.
(A) Somatostatin; (B) octreotide; (C) ^{111}In-DTPA-labeled octreotide.

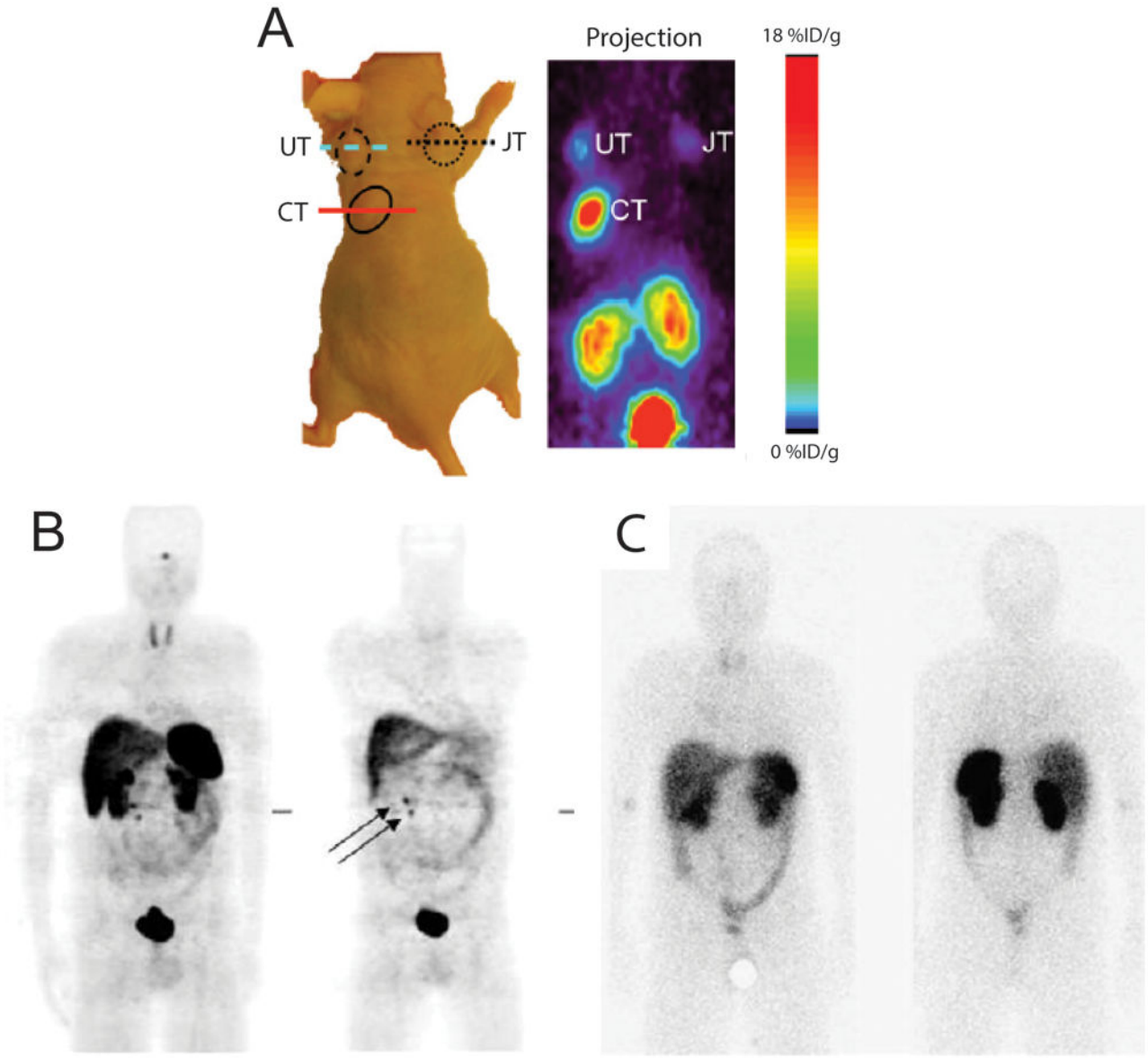

Figure 5.

(A) Small-animal PET images using ^{68}Ga-DOTATOC showing tumor delineation in a mouse bearing subcutaneous xenografts that express different levels of SSTr2 (CT = C6-SSTr2, JT = Jurkat-SSTr2, and UT = U87-SSTr2; SSTr2 expression CT > UT > JT). This research was originally published in the *Journal of Nuclear Medicine* (see ref 131). Copyright 2011 Society of Nuclear Medicine and Molecular Imaging, Inc. (B) ^{68}Ga-DOTATOC PET images (left, anterior view; right, posterior view) of a patient with SSTr(+) abdominal lymph nodes (arrows). (C) SPECT images of ^{111}In-DTPA-octreotide in the same patient displaying reduced resolution. Adapted and reprinted with kind permission from ref 156. Copyright 2007 Springer Science + Business Media.

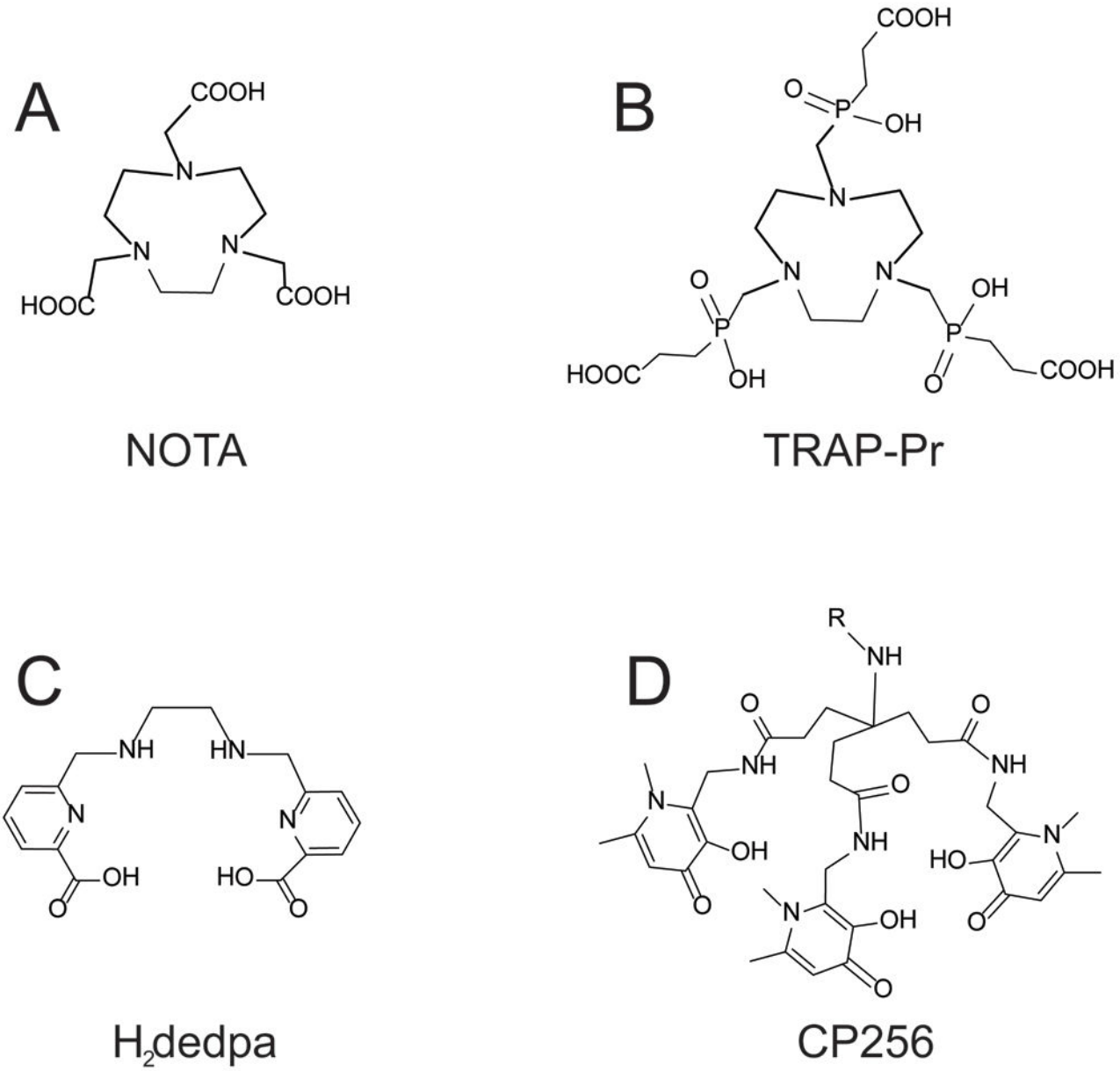

Figure 6.

Macrocyclic ligands NOTA (A) and TRAP-Pr (B) and acyclic chelators H_2dedpa (C) and CP256 (D) have better Ga^{3+}-chelating properties than DOTA based on thermodynamic stability and apotransferrin ligand-exchange tests.

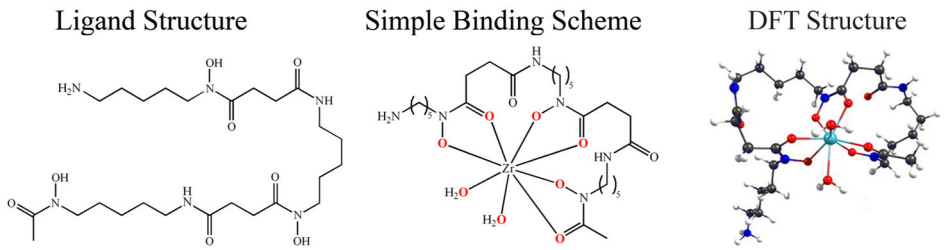

Figure 7.

(A) Structure of DFO. (B) Simple binding scheme of Zr^{4+} with DFO. (C) Calculated DFT structure of Zr^{4+} with DFO. Adapted with permission from ref 11. Copyright 2012 Elsevier Publishing Group, Inc.

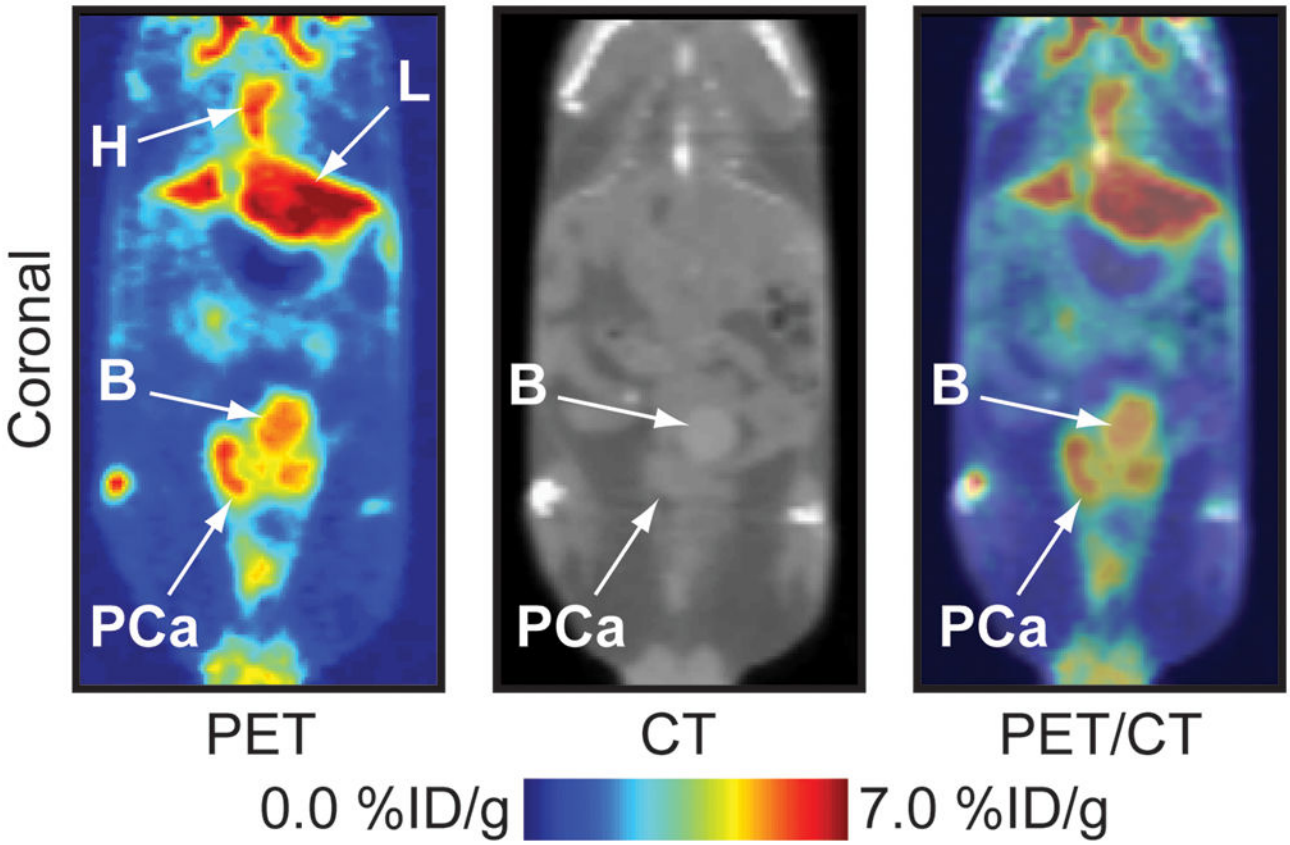

Figure 8.

Representative coronal slices of a coregistered PET/CT showing the distribution of ^{89}Zr-Tf in a genetically engineered mouse with prostate-specific overexpression of MYC. The animal was 12 months old, a time point at which invasive adenocarcinoma had developed. The images were acquired 16 h postinjection of ^{89}Zr-Tf. Ex vivo analysis confirmed uptake of the radiotracer in malignant tissue. Abbreviations: H = heart; L = liver; B = bladder; PCa = prostate cancer. This research was originally published in *Nature Medicine* (see ref 231). Copyright 2012 Nature Publishing Group, Inc.

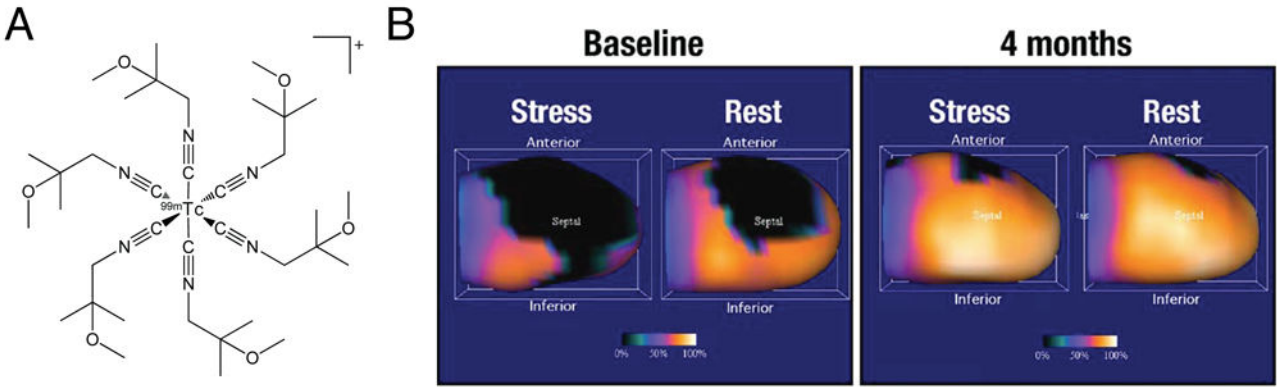

Figure 9.

(A) Structure of ^{99m}Tc-sestamibi. (B) ^{99m}Tc-sestamibi SPECT scintigraphy looking at myocardial perfusion. A 54-year-old man with acute anterior myocardial infarction initially presented with a perfusion defect of the anteroseptal and apical territories of the heart (left), but 4 months later, perfusion defect and ischemia were significantly reduced (right). Adapted and reprinted with kind permission from ref 244. Copyright 2010 Springer Science + Business Media.

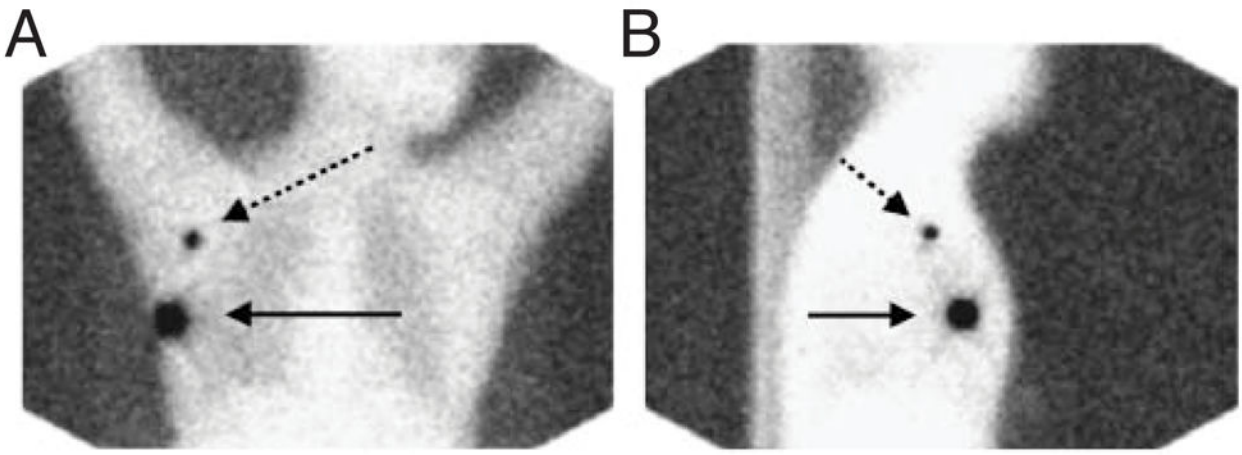

Figure 10.

^{99m}Tc-sulfur-colloid SPECT lymphoscintigraphy. Anterior (A) and right-lateral (B) transmission images obtained 30 min after injection of ^{99m}Tc-sulfur-colloid into the left breast show the injection site (solid arrow) and focal uptake (dashed arrow) in the sentinel node in the right axilla. This research was originally published in the *Journal of Nuclear Medicine* (see ref 263). Copyright 2006 Society of Nuclear Medicine and Molecular Imaging, Inc.

Table 1

Physical Properties of Some Common PET Radiometals[a]

isotope	half-life/h	source	production reaction	decay mode (% branching ratio)	E_{β^+}/keV	abundance, I_{β^+}/%	E_γ/keV (intensity, I_γ/%)	relevant oxidation states	common coordination numbers
^{64}Cu	12.7	cyclotron	^{64}Ni(p,n)^{64}Cu	$\varepsilon + \beta^+$ (61.5)	278.2(9)	17.60(22)	511.0 (35.2)	1+, 2+	4, 5, 6
				β^+ (17.6)					
				β^- (38.5)					
^{68}Ga	1.1	generator	^{68}Ge/^{68}Ga	$\varepsilon + \beta^+$ (100)	836.02(56)	87.94(12)	511.0 (178.3)	3+	4, 5, 6
				β^+ (89.1)					
^{86}Y	14.7	cyclotron	^{86}Sr(p,n)^{86}Y	$\varepsilon + \beta^+$ (100)	535(7)	11.9(5)	443.1 (16.9)	3+	8, 9
				β^+ (31.9)			511.0 (64)		
							627.7 (36.2)		
							703.3 (15)		
							777.4 (22.4)		
							1076.6 (82.5)		
							1153.0 (30.5)		
							1854.4 (17.2)		
							1920.7 (20.8)		
^{89}Zr	78.4	cyclotron	^{89}Y(p,n)^{89}Zr	$\varepsilon + \beta^+$ (100)	395.5(11)	22.74(24)	511.0 (45.5)	4+	8
				β^+ (22.7)			909.2 (99.0)		

[a] Unless otherwise stated, standard deviations are given in parentheses (IT = isomeric transition; ε = electron capture).[208]

Table 2

Physical Properties of Some Common SPECT Radiometals[a]

isotope	half-life/h	source	production reaction	decay mode (% branching ratio)	E_γ/keV	abundance, I_γ/%	relevant oxidation states	common coordination numbers
^{67}Ga	78.2	cyclotron	^{nat}Zn(p,x)^{67}Ga	ε (100)	91.265(5)	3.11(4)	3+	4, 5, 6
			^{68}Zn(p,2n)^{67}Ga		93.310(5)	38.81(3)		
					184.576(10)	21.410(10)		
					208.950(10)	2.460(10)		
					300.217(10)	16.64(12)		
					393.527(10)	4.56(24)		
^{99m}Tc	6.0	generator	^{99}Mo/^{99m}Tc	β^-(0.0037)	140.511(1)	89.06	1− to 7+	4, 5, 6
				IT (99.9963)				
^{111}In	67.3	cyclotron	^{111}Cd(p,n)^{111}In	ε (100)	171.28(3)	90.7(9)	3+	5, 6, 7, 8
					245.35(4)	94.1(10)		

[a] Unless otherwise stated, standard deviations are given in parentheses (IT = isomeric transition; ε = electron capture).208